Urban Climate 62 (2025) 102507

Contents lists available at ScienceDirect

Urban Climate

journal homepage: www.elsevier.com/locate/uclim

Adaptation and mitigation of outdoor heat stress and building energy consumption during a heat wave in Nicosia, Cyprus

Giandomenico Vurro [a,*], Alberto Martilli [b], Panos Hadjinicolaou [a], Salvatore Carlucci [c], Jacobo Gabeiras Penas [d], Katiana Constantinidou [a], Jos Lelieveld [a,e]

[a] The Cyprus Institute, CARE-C, Nicosia, Cyprus
[b] CIEMAT, Atmospheric Modelling Group, Madrid, Spain
[c] University of Insubria, Department of Theoretical and Applied Sciences, Varese, Italy
[d] University of Grenoble Alpes, Grenoble, France
[e] Max Planck Institute for Chemistry, Mainz, Germany

ARTICLE INFO

Keywords:
Urban climate
Multilayer urban scheme
EMME region
Adaptation strategies
Mitigation strategies
Model performance/evaluation
WRF model

ABSTRACT

Cities in the Eastern Mediterranean and Middle East region face rising temperatures and intensifying heatwaves that are amplified by the urban heat island effect. These challenges pose significant threats to human health, agriculture, and the water–energy nexus, emphasizing the need for in-depth analysis and effective mitigation strategies at the urban scale. To address this need, we model the effects of seven interventions over 19 days, from July 23rd to August 10th, 2021, during a heatwave in Nicosia, Cyprus. We assess three key outcomes using the Weather Research and Forecasting (WRF) model coupled with the multilayer Building Energy Parameterization/Building Energy Model (BEP/BEM) scheme: 2m air temperature, outdoor heat stress, and air-conditioning energy use. Our results demonstrate that urban trees are the most effective single intervention, reducing energy consumption by approximately 46% and decreasing heat stress-degree hours by 20–25 h over the analyzed period. The combined implementation of cool roofs and urban trees proved to be the most effective overall, reducing energy consumption by over 50% and lowering 2m air temperatures by up to 1.2 °C during the day. A promising adaptive mitigation strategy emerged through the integration of photovoltaic panels and urban trees, which reduced heat stress while generating energy that significantly contributes to cooling demands. The efficacy of these interventions varied with urban geometry, with maximum benefits in areas characterized by medium building heights and densities. These findings offer guidance for developing urban climate resilience strategies in semi-arid regions, underscoring the importance of location-specific application of heat adaptation and mitigation measures.

1. Introduction

In recent decades, the urban population has grown drastically worldwide. While it was close to 1 billion in 1960, it grew to 4.1 billion in 2017, corresponding to 55% of the world population. Along with this population increase, the density of cities has also reached unprecedented levels (Santamouris, 2023). Replacement of natural surfaces with light-absorbing materials, lack of green

* Corresponding author.
E-mail address: g.vurro@cyi.ac.cy (G. Vurro).

https://doi.org/10.1016/j.uclim.2025.102507
Received 8 November 2024; Received in revised form 17 January 2025; Accepted 11 June 2025
Available online 12 July 2025

spaces, increasing urbanization and evapotranspiration, and the critical amount of anthropogenic heat released into the atmosphere have contributed to urban temperatures increasing, adding to urban warming the urban heat island effect causing these areas to experience higher temperatures than their rural counterparts, especially during heat waves (Cartalis et al., 2001; Santamouris, 2001; Oke et al., 2017).

The consequences are particularly severe in the Eastern Mediterranean and Middle East (EMME) region, where urbanization trends intensify climate change impacts. The EMME region is recognized as a "climate change hotspot", with temperatures rising almost twice as fast as the global average and increasingly frequent and intense heatwaves expected in the coming decades (Lelieveld et al., 2012). For instance, in Cyprus, historical analysis has shown a statistically significant increase in temperature trends (0.4 °C–0.6 °C per decade), especially during the summer and spring months (Zittis et al., 2022). Future projections indicate that under high emission scenarios, the island could experience an annual temperature increase of over 4 °C by the end of the 21st century, along with a significant reduction in rainfall, up to 30% less than current levels (Lazoglou et al., 2024).

Recent studies have highlighted the compounding effects of climate change and urbanization in the Middle East and North Africa (MENA) region. Hadjinicolaou et al. (2023) found that urban stations in MENA region exhibited temperature trends 0.1 °C per decade higher than rural stations from 1981–2020. Tzyrkalli et al. (2024) identified consistent upward trends in the urban heat island effect across MENA cities, particularly at night, further exacerbating the impacts of regional warming. Furthermore, the amplified warming in the EMME region poses serious threats to human health, agriculture, water resources, and the energy sector. Studies have highlighted the growing incidence of heat stress and related health issues, with significant correlations between high temperatures, hospital admissions, and mortality in regions like Cyprus (Lubczyńska et al., 2015; Kekkou et al., 2023). These trends highlight the urgent need for targeted adaptation and mitigation measures to counteract the effects of urban overheating and climate change (Simpson et al., 2024).

In response to these challenges, the research community has shown increased interest in cities and urban climates to explore climate adaptation and mitigation strategies that can tackle the challenges of climate change in urban environments. Notably, these strategies aim to reduce air temperature at the city scale since, during hot periods, increased likelihood of thermal discomfort and higher mortality rates are observed (Heaviside et al., 2016; Salmond et al., 2016; Brousse et al., 2023; Iungman et al., 2023). Different active and passive strategies have been proposed to counteract the adverse effects of urban overheating on public health and indoor and outdoor comfort. Santamouris (2019) identified four major intervention clusters to counterbalance the urban overheating. The solutions can be classified according to their capacity to increase the albedo of building façades and roofs, provide shade, improve vegetation coverage and green spaces, enhance natural ventilation, and dissipate excess heat to low-temperature environmental sinks without needing external energy (e.g., electricity, natural gas, mechanic work). Among those measures capable of directly reducing temperatures (e.g., outdoor air temperature and surface temperature), increased urban vegetation, green roofs, or cool roofs are the most adopted. As it concerns active technologies, i.e., solutions that transform incoming radiation into energy or mechanically change temperatures, air conditioning (AC) is one of the most adopted to protect from extreme heat. However, it commonly requires a significant amount of energy, contributing to greenhouse gas emissions and exacerbating climate change (Salamanca et al., 2014; Sharma et al., 2016; Santamouris et al., 2017; Stone et al., 2021; Brousse et al., 2023). In addition, photovoltaic panels (PV) deserve particular attention. Although they are primarily considered renewable energy sources, they can also be regarded as passive–active solutions for influencing the outdoor and indoor air by increasing the albedo of the roofs and converting the incoming solar radiation into electricity to power the AC system (Salamanca et al., 2016; Ma et al., 2017; Brousse et al., 2023). Active and passive strategies have mainly been investigated in the literature in recent years, and their effect has been discussed in different case studies. Several have focused on applying at least one of the abovementioned strategies on the building scale (Zinzi and Agnoli, 2012; Kolokotsa et al., 2013; Piselli et al., 2019; Samaro et al., 2024). However, as Zonato et al. (2022) stated, the results obtained on the building scale cannot be directly applied to evaluate mitigation at the city scale because the impact of these solutions depends on different variables such as urban geometry, thermal properties of building materials, and climatic conditions. Therefore, a different approach is required.

Following this view, several recent studies exploited mesoscale meteorological models to analyze the impact of the adaptation strategies at the city scale. For instance, Li et al. (2014) investigated to what extent cool and green roofs were effective in mitigating at the city scale the urban overheating in the Baltimore–Washington metropolitan area using the Weather Research and Forecasting (WRF) model coupled with the Princeton Urban Canopy Model (PUCM). Broadbent et al. (2020) incorporated the effect of cool roofs in the multilayer Building Effect Parameterization (BEP) (Martilli et al., 2002) to examine their cooling impacts at the pedestrian level in Atlanta, Detroit, and Phoenix cities in the USA, while Brousse et al. (2023) employed the WRF Building Effect Parameterization-Building Energy Model (BEP-BEM) (Salamanca et al., 2010; Salamanca and Martilli, 2010) mesoscale model to investigate the impacts of the building- and street-level interventions on air temperature at the urban scale in the Great London Authority area.

Nevertheless, no single heat adaptation strategy fully addresses all relevant considerations. For instance, studies indicate that while cool roofs effectively reduce air temperature and air conditioning (AC) energy use (Broadbent et al., 2020; Viguié et al., 2020), they do not provide shade for pedestrians. Similarly, while street trees can substantially mitigate outdoor heat stress (Lee et al., 2016; Zölch et al., 2016; Aminipouri et al., 2019; Geletič et al., 2022), they may also increase street-level air pollution through inhibited mixing (Rui et al., 2019) and organic aerosol emissions (Kulmala et al., 2013). Furthermore, PV roofs that generate electricity to potentially power AC systems have ambiguous effects on air temperature (Sailor et al., 2021). Oke (1988) and Martilli (2014)'s work has shown that different urban morphologies and vegetation levels can involve trade-offs between thermal comfort, air quality, and energy use. Additionally, the background climate influences urban heat adaptation strategies, suggesting that distinct urban configurations in varying climatic contexts may respond differently to each strategy (Li et al., 2014; Tewari et al., 2019; Wang et al., 2020). Consequently, there is a need to evaluate adaptation measures across diverse neighborhoods and climates.

Therefore, despite the increasing application of such approaches globally, large-scale controlled experiments of urban interventions and assessments of the performance of these strategies are still rare in the EMME region, and given the fact that the region has been labeled as a "climate change hotspot" (Giorgi, 2006; Lelieveld et al., 2012; Zittis and Hadjinicolaou, 2017; Cramer et al., 2018; Zittis et al., 2022), it is of great importance to investigate to what extent these strategies can help to counteract the effect of urban overheating.

To address this gap, following evidence from the literature, this study employs detailed urban climate modeling to quantify the impacts of adaptation and mitigation strategies, including cool roofs, green roofs, increased urban tree canopy, and photovoltaic roofs, on air temperature, outdoor heat stress, and building energy consumption during a heat wave in the semi-arid environment of Nicosia, Cyprus. More specifically, our research questions are: *How do cool roofs, green roofs, urban trees, and photovoltaic panels perform during a heat wave in Nicosia, Cyprus? How do these strategies affect 2m air temperature, outdoor heat stress, and AC energy use? Can synergistic effects of combined strategies provide more significant benefits than individual implementation? To what extent does the strategies' impact depend on the building's geometry?* Our methodology considers the urbanized WRF mesoscale model to obtain information on outdoor climate and building energy use during the simulation period. To assess outdoor heat stress, we adopt the Universal Thermal Comfort Index (UTCI), which captures the physiological impacts of radiant temperature, humidity, wind speed, and air temperature. The simulations of adaptation strategies illustrate maximum strategies and potential applications to group their possible effects.

This study aims to bridge significant gaps in urban climate research by focusing on the dual aspects of heat stress and building energy use within the specific context of the Eastern Mediterranean and Middle East (EMME) region. By analyzing the effects of various adaptation and mitigation strategies across different urban densities and leveraging detailed, high-resolution data on Nicosia's urban features, this work provides a nuanced understanding of the interplay between urban design, thermal comfort, and energy demand. Although some strategies evaluated may be challenging to implement on a large scale, the insights gained can guide policymakers in formulating climate resilience measures suited to the semi-arid environments of the EMME region. This multifaceted approach offers a novel contribution to the field by moving beyond simplistic assessments of temperature extremes.

The paper follows this structure: Section 2 provides a description of the region of interest and case study along with the model set-up adopted to run the simulations, information about the urban morphology of the case study, and the observational dataset used to validate the model and evaluate its performance. Section 3 describes the results of the various simulations, 4 discusses the findings, and finally, in Section 5, conclusions are derived.

2. Methods and data

2.1. Region of interest and case study

This study uses a comprehensive three-dimensional urban scheme to investigate the impact of different cooling strategies on the air temperature of the city of Nicosia. The city is situated near the Mesaoria plain's center, on the banks of the Pedieos River, in the eastern part of the Mediterranean island of Cyprus. The island is located in the Eastern Mediterranean at the crossroads of three continents: Europe, Asia, and Africa. After Sicily and Sardinia, Cyprus is the third-largest island in the Mediterranean, covering an area of approximately 9251 km^2.

The island is characterized by mild, rainy winters and long, hot, and dry summers (Köppen, 1884; Kottek et al., 2006; Hadjinicolaou et al., 2011; Zittis et al., 2020; Castaño-Rosa et al., 2021), while, according to the Köppen–Geiger system, some parts of the island are classified as hot and dry (Köppen, 1884; Kottek et al., 2006; Peel et al., 2007; Zittis et al., 2017). Annually, the region experiences over 300 days of sunshine. In July, temperatures range from 22 to 37 °C in inland areas, from 21 to 32 °C along the southern and eastern coastlines, between 20 and 30 °C at western and northern parts, and from 17 to 28 °C in mountainous regions with an elevation above 1000 m (Tymvios et al., 2018).

The surrounding areas of the city exhibit varying land use patterns, including urban developments, agricultural lands, and natural vegetation. The region's topography consists of undulating terrain with hills to the north and south, significantly influencing local weather patterns and airflow. The city of Nicosia has a population of approximately 262 thousand people, making it the largest city on the island. The area covers about 111 km^2, resulting in a population density of around 3150 people per square kilometer (Statistical Service of Cyprus, 2023).

Our case study focuses on the period from July 23rd, 2021, to August 10th, 2021. During this period, a 12-day heatwave event occurred (defined here as a period of three or more consecutive days with maximum temperature exceeding the 95th percentile Zittis et al., 2021) from July 27th to August 7th, with temperatures exceeding 40 °C on several days, with a peak of 44.3 °C on August 4th.

2.2. Observational dataset

The observational meteorological data for three different locations in the Greater Nicosia Area were provided by the Cyprus Department of Meteorology. Specifically, the meteorological stations are Nicosia Downtown, an urban station (35.1653° N, 33.3550° E), Athalassa, a suburban station (35.1444° N, 33.4033° E), and Astromeritis, a rural station (35.1327° N, 33.0198° E). These stations belong to the Department of Meteorology network of automatic stations and provide data from July 24th, 2021, to August 10th, 2021.

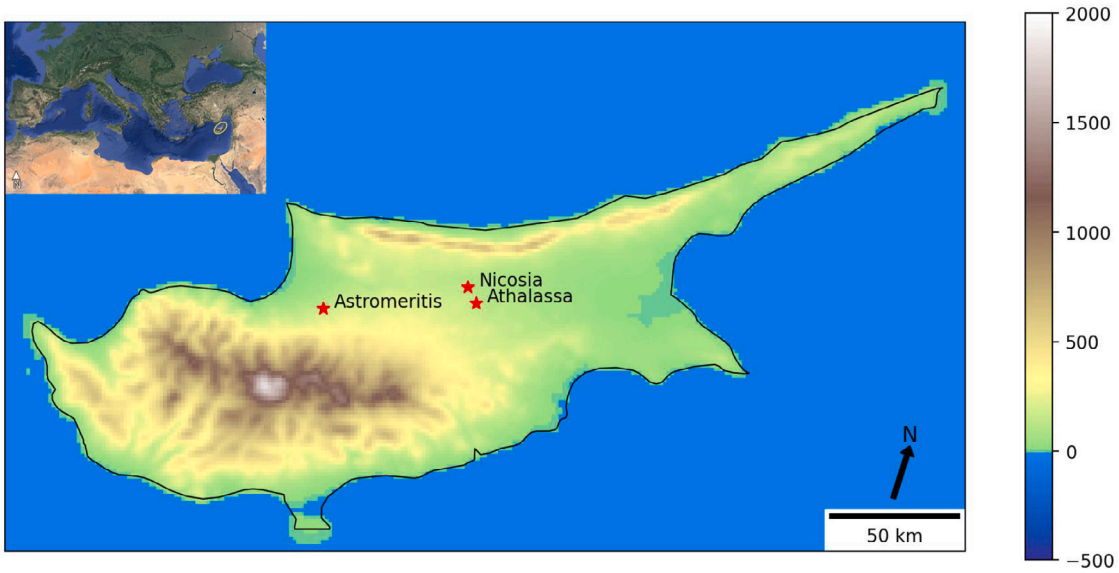

Fig. 1. Distribution of the meteorological stations in and around the Greater Nicosia Area. The three stations in red are those used in this study. The insert shows Cyprus's geographical location (yellow circle) in the eastern Mediterranean.

Table 1
Meteorological stations.

Station number	Station name	Distance fromNicosia (km)	Elevation (m)	Longitude (°E)	Latitude (°N)
1415	Astromeritis	30.84	159	33.02	35.13
1668	Athalassa (Environmental)	4.84	154	33.40	35.14
1640	Nicosia		162	33.35	35.16

The observational database includes mean, maximum, and minimum 2m air temperature, relative humidity, and 10 m wind speed and direction at 1-hour resolution. This data has been processed to create daily and diurnal averages of all parameters. The spatial distribution of the stations is illustrated in Figs. 1 and 3, and Table 1 summarizes the characteristics of each station in terms of official names, latitude, longitude, and elevation above sea level. Notably, the urban station did not have wind speed and direction data due to equipment unavailability. Following recommendations from prior research Pyrgou et al. (2020), the wind profile from the suburban station, located 4.6 km away, was used as a substitute for the urban station.

2.3. WRF implementation

2.3.1. Model set-up

The Advanced Research version of the Weather Research and Forecasting (WRF-ARW) model, version 4.5.1 (Skamarock et al., 2019, 2021), is used to run simulations over the Greater Nicosia Area with a horizontal resolution of 1 km and 57 vertical levels, with the top one set at 50 hPa and the lowest considered with a 10-meter thickness. The WRF model is a highly adaptable atmospheric simulation system that can be used effectively at various scales, from regional to urban. This is due to its nesting features and the ability to be coupled to an urban canopy parameterization (UCP) (Chen et al., 2011).

In this research, the WRF model with the BEP-BEM multilayer scheme is used to enhance the representation of physical surface energy interactions within urban areas, wind drag effects, and spatial variations in urban environments. The WRF configuration adopted for this study consists of three nested domains with horizontal resolutions of 12 km, 3 km, and 1 km. The domains were selected to include all the geographical features that might have a synoptic or regional influence on the Greater Nicosia Area meteorology. The outermost domain encompasses the EMME region. The second domain covers the island of Cyprus, part of the Atlas Mountains, and part of the Levant region. Finally, the innermost domain considers the entire island exclusively (Fig. 2).

All the simulations cover the period from 00:00 EET on July 23rd, 2021, to 00:00 EET on August 10th, 2021, allowing us to simulate all the heat wave events during that period. The first 24 h have been considered as a spin-up period. Furthermore, only the innermost domain simulations are evaluated against the observed data. The corresponding model evaluation against the urban meteorological stations is found in Supplementary Sect. 1.

Further details regarding the model characteristics and configurations, such as the domain resolution and physical parameterizations, are shown in Table 2.

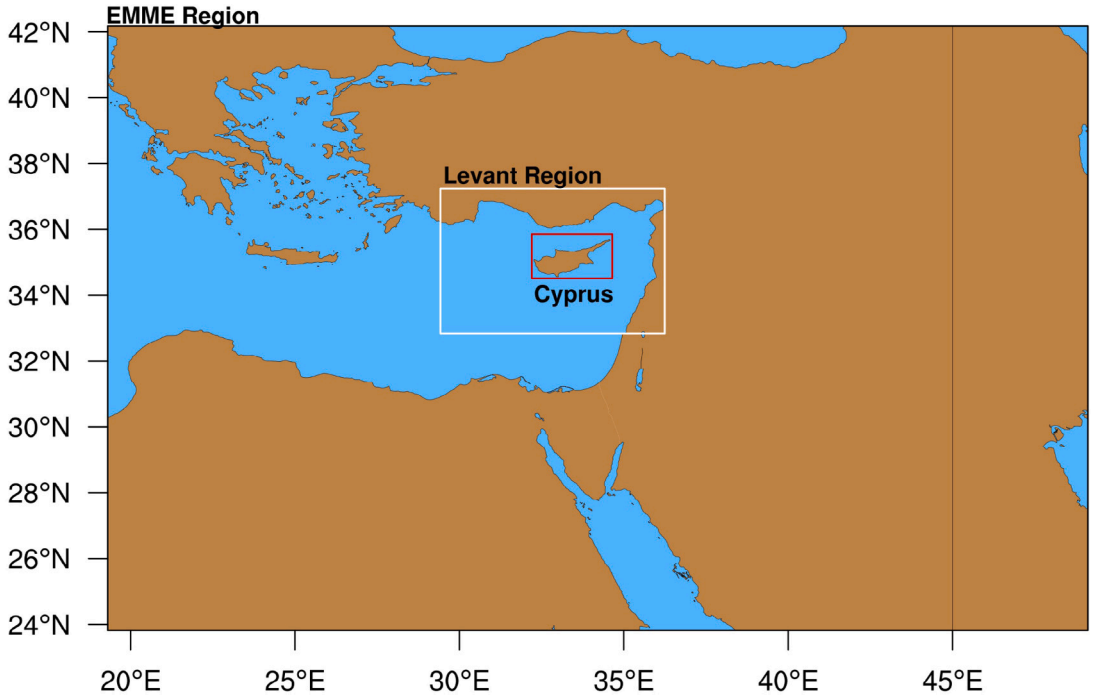

Fig. 2. Domains of the WRF model for this study: EMME Region (d01), Levant Region (d02), and Cyprus (d03) with 12 km, 3 km, and 1 km horizontal resolution, respectively.

Table 2
Model characteristics and configurations.

Resolution and initial conditions	
Horizontal resolution	12 km × 12 km; 3 km × 3 km; 1 km × 1 km
Vertical layers	57
Top of the atmosphere	50 hPa
Initial conditions	ERA5 (Hersbach et al., 2020) with 31 km horizontal resolution,137 vertical levels, and hourly output
Physics parameterizations	
Microphysics	WRF Single-Moment 6-Class Scheme (Hong and Lim, 2006)
Shortwave and longwave radiation	RRTMG scheme (Iacono et al., 2008)
Cumulus	Kain-Fritsch scheme (only d01 and d02) (Kain, 2004)
Surface	Noah Land Surface Model (Chen and Dudhia, 2001)
UCP	Building Effect Parameterization-Building Energy Model (BEP-BEM) (Martilli et al., 2002)
PBL	Bougeault and Lacarrere (Bougeault and Lacarrere, 1989)
Surface layer	Revised MM5 Monin–Obukhov scheme

2.3.2. Gridded urban parameters

Urban canopy models like BEP-BEM usually rely on Local Climate Zones (LCZs) to assign urban parameters through predefined tables. This approach categorizes areas based on broad thermal and aerodynamic characteristics, such as conductivity and resistance, which were then applied uniformly to all grid cells within each LCZ. However, recent versions of the model can now take certain parameters directly at the level of each grid cell, enabling finer-scale representation of urban morphology. The urban parameters corresponding to building plan area fraction, building surface area to plan area ratio, and weighted mean building height were computed by integrating three complementary datasets: the Microsoft Building Footprints dataset (Microsoft, 2024), the World Settlement Footprint 3D (WSF3D) dataset (Marconcini et al., 2021), and the World Urban Fraction dataset (Patel and Roth, 2022). The last two datasets were extracted for the area of interest with the *wrfup* python package (Gabeiras, 2024). For parameters that are not available at the grid-cell level, such as material properties, the LCZ-based approach remains essential. By combining these two approaches, the model leverages both fine-scale variability and broader land use classifications, ensuring a more accurate representation of the urban environment.

The Microsoft Building Footprints dataset provides the shapes of each building in the island, defined by their vertices in the form of a vector file. From this, the planar surface area (A_P) and perimeter of each building can be extracted. However, it does not include information about building heights. The WSF3D dataset is a raster file with a resolution of 90 meters that provides the mean building height (H) within each grid cell, though it lacks detailed information about individual building shapes. The World

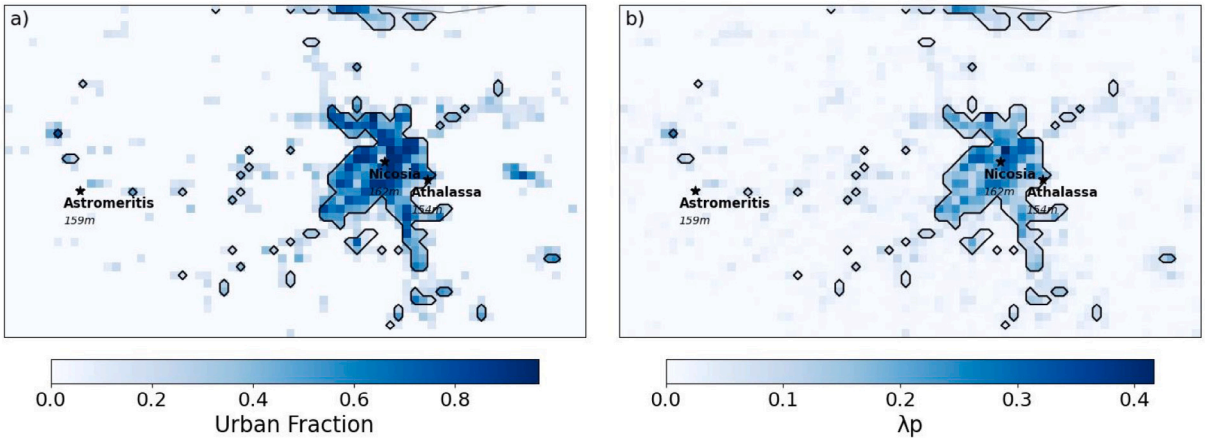

Fig. 3. Details of (a) urban fraction, (b) λ_p, and locations of the meteorological stations.

Urban Fraction dataset, with a resolution of 100 m, quantifies the proportion of built-up area in each grid cell and was averaged to 1-km resolution to match the model domain.

The mean building heights from the WSF3D dataset were assigned to each building based on the grid cell with the largest overlap. The necessary urban parameters—the building plan area fraction (λ_p), the building surface area to plan area ratio (λ_b), and the weighted mean building height (h_m)—were calculated at the level of each grid cell as follows:

$$\lambda_p = \frac{\sum_i A_{P,i}}{\lambda_F \cdot A_T} \tag{1}$$

$$\lambda_b = \frac{\sum_i (A_{W,i} + A_{P,i})}{\lambda_F \cdot A_T} \tag{2}$$

$$h_m = \frac{\sum_i (H_i \cdot A_{P,i})}{\sum_i A_{P,i}} \tag{3}$$

In these equations:

- λ_p is the building plan area fraction, quantifies the planar density of buildings within the built-up portion of the grid cell.
- λ_b is the building surface area to plan area ratio, reflects the three-dimensional complexity of the urban fabric.
- h_m is the weighted mean building height, representing the average height of buildings in the grid cell.
- λ_F is the urban fraction, derived from the World Urban Fraction dataset and averaged to 1-km resolution.
- A_T is the total area of the grid cell.
- $A_{P,i}$ is the planar surface area of each building (equivalent to the roof area).
- $A_{W,i}$ is the wall area of each building, calculated as $A_W = \text{Perimeter} \cdot H$.
- H_i is the height of each building.

2.3.3. Local climate zone based urban parameters

Thermal properties of building components, which are not available at the grid-cell level, were assigned to the model through the Local Climate Zones (LCZs) framework. These properties were first identified through site visits and the analysis of construction ages and building archetypes and, then, assigned to the building models of the area of study distinguishing between those within the ancient Venetian walls in the old town and those outside. Specifically, based on information provided in Fokaides et al. (2014), we assigned thermal characteristics typical of masonry and roof constructions prior to the Energy Performance of Buildings Directive (EPBD) adoption to buildings in old town while assigning post-EPBD adoption characteristics to buildings outside. Detailed information about materials, including thicknesses, thermal conductivity (λ), and resistance (R), can be found in Tables 3, 4, 5, and 6.

2.4. Cooling strategies

We establish eight passive strategies that could be implemented across Nicosia. In similar research contexts, the selected strategies have been demonstrated to reduce urban heat and improve thermal comfort effectively (Brousse et al., 2023; Jiang et al., 2025). Most of these strategies involve rooftop interventions, and each intervention is evaluated against a control run that did not consider any intervention. Thus, the control run serves as a baseline for understanding the influence of urban areas on local climate, allowing us to investigate temperature variability further.

Table 3
Typical masonry construction pre-EPBD. The terms R_{si} (m^2K/W), R_{se} (m^2K/W), and U_{value} (W/m^2K) represent the internal and external surface resistance and the thermal transmittance, respectively.

U_{value} Calculation (External wall) pre-EPBD			
Material (Starting from the inner side)	Thickness (m)	Thermal Conductivity λ (W/mK)	Thermal Resistance R (m^2K/W)
Plaster	0.025	1	0.025
Brick	0.2	0.4	0.5
Plaster	0.025	1	0.025
R_{si} (m^2K/W)			0.13
R_{se} (m^2K/W)			0.04
U_{value} (W/m^2K)	**1.388**		

Table 4
Typical masonry construction post-EPBD. The terms R_{si} (m^2K/W), R_{se} (m^2K/W), and U_{value} (W/m^2K) represent the internal and external surface resistance and the thermal transmittance, respectively.

U_{value} Calculation (External wall) post-EPBD			
Material (Starting from the inner side)	Thickness (m)	Thermal Conductivity λ (W/mK)	Thermal Resistance R (m^2K/W)
Plaster	0.025	1	0.025
Perforated Thermal Brick	0.3	0.2	1.5
Plaster	0.025	1	0.025
R_{si} (m^2K/W)			0.13
R_{se} (m^2K/W)			0.04
U_{value} (W/m^2K)	**0.581**		

Table 5
Typical roofs construction pre-EPBD. The terms R_{si} (m^2K/W), R_{se} (m^2K/W), and U_{value} (W/m^2K) represent the internal and external surface resistance and the thermal transmittance, respectively.

U_{value} Calculation (Roof) pre-EPBD			
Material (Starting from the inner side)	Thickness (m)	Thermal Conductivity λ (W/mK)	Thermal Resistance R (m^2K/W)
Trowel	0.01	0.8	0.0125
Reinforced Concrete	0.15	2.5	0.06
Screed	0.1	1.35	0.074
Waterproofing Layer	0.005	0.23	0.021
R_{si} (m^2K/W)			0.1
R_{se} (m^2K/W)			0.04
U_{value} (W/m^2K)	**3.252**		

Table 6
Typical roofs construction post-EPBD. The terms R_{si} (m^2K/W), R_{se} (m^2K/W), and U_{value} (W/m^2K) represent the internal and external surface resistance and the thermal transmittance, respectively.

U_{value} Calculation (Roof) post-EPBD			
Material (Starting from the inner side)	Thickness (m)	Thermal Conductivity λ (W/mK)	Thermal Resistance R (m^2K/W)
Trowel	0.01	0.8	0.0125
Reinforced Concrete	0.15	2.5	0.06
Ins. Material (polystyrene)	0.1	0.03	3.333
Screed	0.1	1.35	0.074
Waterproofing Layer	0.005	0.23	0.021
R_{si} (m^2K/W)			0.13
R_{se} (m^2K/W)			0.04
U_{value} (W/m^2K)	**0.274**		

Notably, we calculate daily 2m air temperature reductions and their associated standard deviations (σ) over the simulation period, quantitatively measuring model uncertainty. Owing to computational limitations, a deterministic modeling approach was deemed more feasible than an ensemble methodology. Nevertheless, the literature indicates that temperature measurements generally exhibit lower internal variability compared to precipitation (Giorgi and Bi, 2000; Alexandru et al., 2007; Lavin-Gullon et al., 2021; Petrovic et al., 2024), thus bolstering the reliability of single-simulation analyses focused on temperature-related outcomes.

At the same time, all the following scenarios assess the impact of each intervention on this urban climate. It is worth mentioning that all the simulations take into account the activation of the air conditioning to ensure indoor thermal comfort. In particular, the set-point temperature is fixed at 26 °C, and the comfort range varies between ±3.5 °C (Fanger, 1970; ISO7730, 2005; ASHRAE, 2017).

All the simulations model the maximum possible implementation of each strategy to delineate their potential impact. Furthermore, for all the scenarios, including the baseline one, we evaluate the outdoor thermal comfort by calculating the Universal Thermal Comfort Index (UTCI) using the $WRF_{comfort}$ model (Martilli et al., 2023), and the building energy consumption using the BEM component.

Following, a brief description of the standalone strategies is provided:

1. **Photovoltaic panels** (PVs) We considered the WRF BEP-BEM PV roof module developed by Zonato et al. (2022). We set a 100% rooftop coverage for each simulation where PVs were included. As provided in the reference paper, we assume an upward emissivity of 0.79 and an efficiency η_{PV} of 19%.
2. **Cool roofs** (CR) Roof albedo is increased to 0.85 in WRF BEP-BEM for cool roof simulations (Brousse et al., 2023). We changed the albedo of all the roofs within the city's urban boundaries. For the control scenario, we adopt a roof albedo of 0.30.
3. **Green roofs** (GR) The green roofs strategy has been included in the simulations adopting the WRF BEP-BEM green roof module of Zonato et al. (2022). As for the PVs strategy, we considered a 100% rooftop grass coverage for Nicosia. In addition, we consider the irrigation of the roofs occurring from 11.00 pm EET to 01.00 am EET each day, for a total of 7.5 mm/day. The control scenario does not assume the implementation of green roofs.
4. **Urban trees** (UT) To estimate the effect of street trees at the city level, we use the WRF BEP-BEM trees module adapted from Stone et al. (2021), Fung et al. (2024) WRF-BEP-Tree model. While the control scenario presents a tree fraction of 20% to represent the existing tree coverage for Nicosia, we increased the fraction to 80% in this scenario, considering a leaf area index (LAI) of 3, considered a reasonable value for urban trees (Fung et al., 2024), and crown height between 5 m and 10 m. This study aims to evaluate the effects of increasing street tree coverage to capture the interactions between buildings and trees. The baseline scenario and street tree simulations include existing trees as represented by the Noah land surface model The additional street trees incorporated into the model are assumed to be unirrigated.

In addition to examining the standalone strategies, we explored the effects of implementing combined strategies. Specifically, we investigated:

- Combination of green roofs with photovoltaic panels ($GRPV$);
- Combination of cool roofs with urban trees ($CRUT$);
- Combination of green roofs with urban trees ($GRUT$);
- Combination of photovoltaic panels with urban trees ($PVUT$).

It is worth mentioning that the combined strategies maintain the same proportional coverage as their standalone counterparts. For instance, when the GRPV (green roof and photovoltaic) approach is implemented, green roofs and photovoltaic panels will occupy 100% of the available rooftop area. In particular, green roofs are located below the photovoltaic panels.

The rationale for assuming full implementation of the proposed strategies is to assess their maximum potential impact. This approach directly compares the strategies under standardized conditions, identifying their advantages, limitations, and optimal solutions. While recognizing that 100% coverage may not be economically feasible, this methodology provides valuable insights that can inform more practical, partial implementations and guide policy decisions.

Previous studies have highlighted the effectiveness of urban adaptation strategies under idealized conditions (Georgescu et al., 2014; Salamanca et al., 2016; Krayenhoff et al., 2018). For example, green and cool roofs have been shown to mitigate urban heat effectively (Sharma et al., 2016; Macintyre and Heaviside, 2019), while targeted and citywide implementations offer additional opportunities for optimization (Broadbent et al., 2020, 2022; Brousse et al., 2023). Although not always practically viable, these comprehensive assessments help pinpoint the most effective strategies for reducing urban heat and improving energy efficiency.

3. Results

3.1. 2m air temperature

The average difference in 2m air temperature, calculated as the scenario run minus the control run, for each strategy allows us to identify the effectiveness of each intervention in reducing temperature. Generally, all strategies except the added PVs reduce the 2m air temperature in the city. In particular, averaged over the 19 days, we found that when comparing rooftop-only strategies, cool roofs reduce temperatures by approximately 0.41 ± 0.12 °C within the Nicosia boundaries, while the combination of cool roofs and trees achieves a more substantial reduction of up to approximately 0.74 ± 0.17 °C. In addition, the reduction of the 2m air temperature, in all scenarios, is much larger during daytime than at night (Supplementary Sect. 2, Figures 9 and 10) when urban surfaces are exposed to high solar radiation and particularly susceptible to interventions involving trees (Fig. 4).

During the day, both cool and green roofs, combined with trees, reduce the temperature by 1.75 ± 0.35 °C and 1.47 ± 0.55 °C, respectively. Though the impact is less pronounced at night, a cooling trend persists along a northwest–southeast axis. This is driven by the prevailing winds from the northwest (Supplementary Sect. 2, Figure 8), which help disperse heat, particularly in areas with lower building density. (Supplementary Sect. 2, Figures 9 and 10).

To better understand the impact of the different strategies, we examined Nicosia's urban geometry. In order to quantify the average effect of the proposed interventions based on the urban configuration, we studied the relationship between the impact of the strategies on the air temperature at 2m, H, and λ_p.

Different bins have been created and analyzed to represent the spatial variability of λ_p and H within the urban area. For λ_p, ranging from 0 to 0.41, four bins are considered: 0.15, 0.25, 0.35, and 0.41. Likewise, we considered three ranges for building

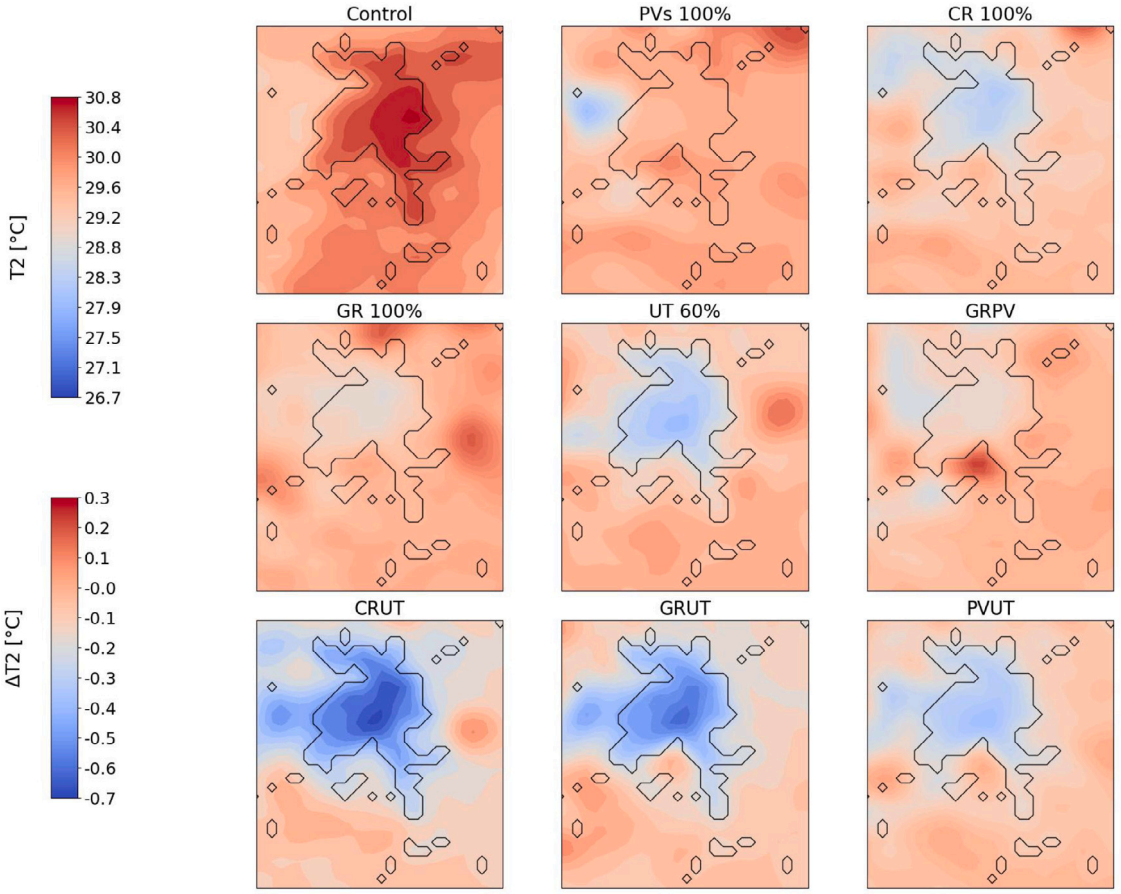

Fig. 4. Average over the 19 days 2m air temperature of the Control run (T2; top left box) and the average difference (ΔT2) of each strategy, Photovoltaic panels (PVs), Cool Roofs (CR), Green Roofs (GR), Urban Trees (UT), Green Roofs combined with Photovoltaic panels (GRPV), Cool Roofs combined with Urban Trees (CRUT), Green Roofs combined with Urban Trees (GRUT), and Photovoltaic panels combined with Urban Trees (PVUT), respectively. Black contours represent WRF urban pixels.

height: 0–5 m, 5–10 m, and 10–15 m. For instance, the 0.15 λ_p bins contain all the buildings with density values between 0 and 0.15. In the same way, the 5 m H bin represents all the buildings with a height between 0 and 5 m.

Fig. 5 shows the average difference of each strategy. The first row of plots considers only the rooftop strategies (PVs, CR, GR, and GRPV), whereas the second considers the presence of trees (UT, CRUT, GRUT, and PVUT). Regarding the displacement of the tallest buildings in the city, they are located in a medium-density area characterized by a λ_p value of 0.35. The most dense area of the city corresponds to the old town, enclosed within the Venetian walls.

As mentioned above, when considering only the rooftop strategies, the most effective strategy is CR, with an average 2m air temperature reduction, over the 19 days, of about 0.35 °C. Almost all the rooftop strategies show negative temperature differences that increase quasi-linearly by increasing the buildings' density and height. An exception is the PVs strategy, which shows a negligible temperature reduction for buildings up to 10 meters tall.

When trees are included, the CRUT strategy is, once again, the one that reduces air temperature the most. It should be noted that the largest reduction in the CRUT strategy occurs for a λ_p value of 0.35 and buildings with a height greater than 5 m. Notably, for buildings between 5 and 10 m in height, an increase in the roof area does not result in enhanced cooling. This can be explained by the fact that as building density increases, the available area for tree planting within each cell decreases. Also, taller buildings already cast significant shadows, reducing the additional shading impact of trees. In general, the effect of interventions, especially for rooftop strategies, diminishes as building height increases.

3.2. Outdoor heat stress

Heat stress has been studied by considering the 50th percentile of the Universal Thermal Comfort Index (UTCI) of the distribution of subgrid scale values obtained with the methodology described in Martilli et al. (2024). In particular, for each simulation, the frequency of hours falling within one of the heat stress categories was calculated and averaged for the whole period. Each heat

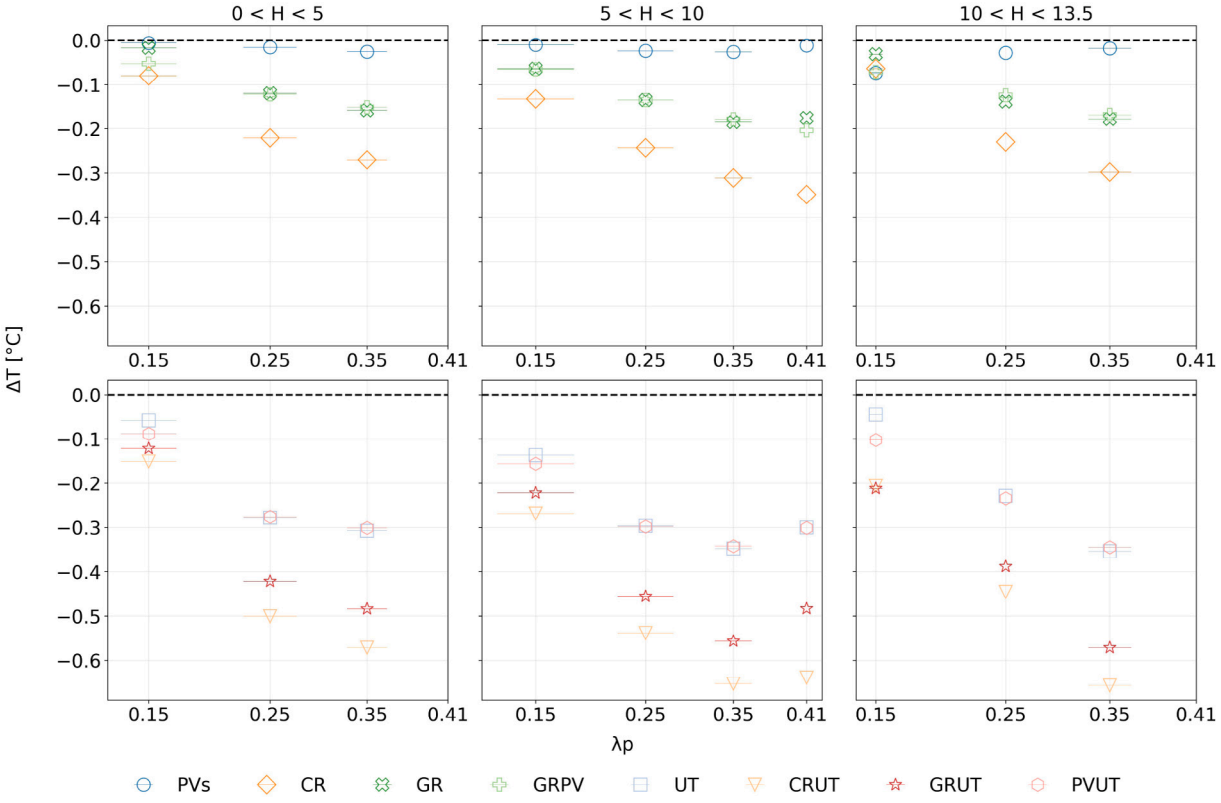

Fig. 5. Average 2m air temperature differences (Y-axis) between each intervention (symbol legend) and the control run for different ranges of building area ratio λ_p (X-axis) and building heights H (left: $0 < H < 5$, middle: $5 < H < 10$, right: $10 < H < 13.5$). Top row: rooftop strategies; bottom row: urban trees.

stress category is characterized by a threshold. In particular, no thermal stress is experienced when the UTCI lies between 9 and 26 °C. Moderate heat stress occurs at UTCI between 26 and 32 °C, while strong heat stress refers to a UTCI between 32 and 38 °C. Very strong heat stress is characterized by a UTCI that ranges between 38 and 46 °C, and finally, extreme heat stress is experienced for UTCI above 46 °C. When adaptation strategies are not considered (control scenario), 32 h (7% of the total period) fall within the category of very strong heat stress, 121 h (26.6%) belong to the category of strong heat stress, 113 h (24.8%) are in the category of moderate heat stress, and 189 (41.5%) are in the category of not thermal stress, for the entire urban area of Nicosia, respectively. Most adaptation strategies analyzed reduce heat stress (Fig. 6). When we focus solely on street trees (UT), they emerge as the most effective strategy for mitigating heat stress. Their shade-providing capability plus the cooling effect from evapotranspiration make them highly effective in reducing UTCI. Under this scenario, the number of hours in very strong heat stress is only 11 (2.4%), with 125 h (27.5%) in strong heat stress, 115 h (25.3%) in moderate heat stress, and 204 h (44.8%) in no thermal stress.

No other strategy is able to reduce heat stress as much as trees. The second best strategy turns out to be cool roofs (CR), which decrease the number of hours to 25 (5.5%), 125 (27.5%), and 108 (23.7%) for very strong heat stress, strong heat stress, and moderate heat stress, respectively, while slightly increase to 197 (43.2%) the hours spent in no thermal stress.

Green roofs (GR) and photovoltaic panels (PVs) are less effective, however, they show comparable results in reducing hours spent in one of the heat stress categories. For instance, when comparing the hours in very strong heat stress for the PV strategy and GR against the control scenario, we find PVs do not reduce heat stress at all, while GR's reduction consists of three hours.

It is important to note that urban trees can be combined with rooftop strategies to achieve even more significant heat stress reduction. The cool roofs combined with urban trees (CRUT) scenario, which combines the air temperature cooling of cool roofs with the shading of street trees, leads to the maximum reduction in heat stress among all the cases investigated.

Analyzing the hourly distribution of the heat stress categories during the 19 days of simulation (Fig. 7), reveals a concentration of the very strong heat stress category during the peak daytime hours. The beneficial effects of the interventions are evident across most strategies. Among the rooftop interventions, cool roofs demonstrate most significant reduction of UTCI by lowering air temperature. However, this strategy shows limited effectiveness in alleviating nighttime heat stress. On the other hand, urban trees prove to be more effective in mitigating very strong heat stress and reducing moderate heat stress at night. Trees provide shade to buildings during the day, resulting in decreased heat storage and reduced longwave emissions, thereby enhancing pedestrian comfort. The combined cool roofs and urban trees (CRUT) scenario best illustrates this synergistic effect. It showcases the trees' capacity to lower pedestrian UTCI during the hottest daytime hours while also providing nighttime benefits. The CRUT strategy demonstrates a

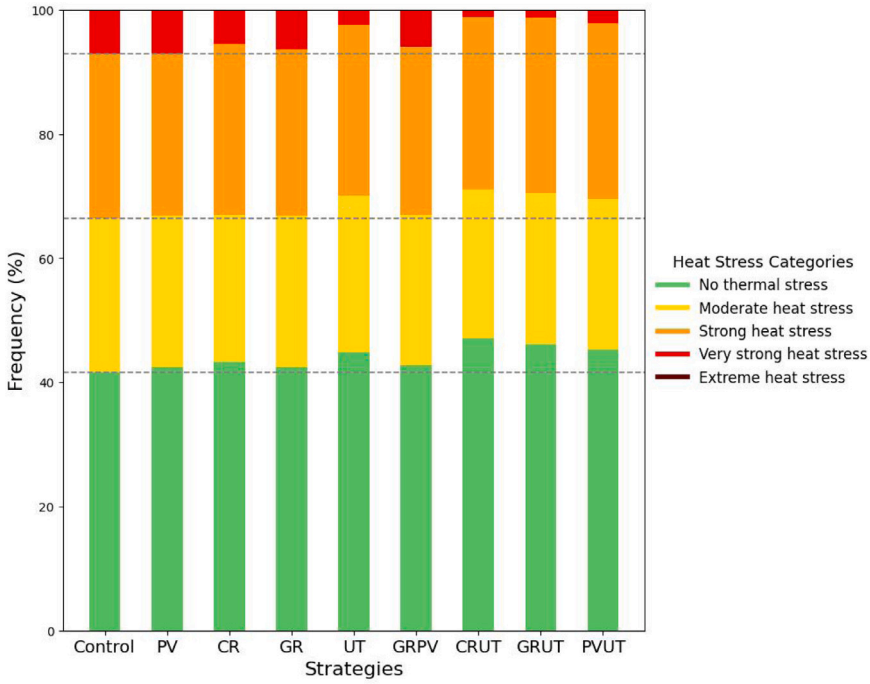

Fig. 6. Frequency of UTCI 50th percentile heat stress categories averaged for the 19 days for each intervention.

reduction of very strong heat stress around 3:00 PM and maintains a reduction of moderate heat stress at night hours, highlighting its round-the-clock effectiveness.

The relationship between UTCI and building density and height indicates that the proximity of buildings, particularly in the most densely built-up areas, generates a beneficial effect due to the building shade. This effect is particularly notable for cool roofs, which emerge as the most effective strategy among rooftop interventions. However, this mitigation effect is even more pronounced at the pedestrian level, where urban trees alone or in combination with cool roofs are considered. Conversely, the mitigation effect is diminished for the tallest buildings when considering standalone strategies or combined approaches.

3.3. AC energy use

Fig. 9 shows the cumulative spatial distribution of AC energy use for the control run and the strategies. The analysis has focused solely on the energy required for cooling and does not account for the energy generated by the photovoltaic systems.

The baseline scenario without mitigation interventions exhibits high energy consumption, particularly in the high-density core of the city, exceeding 2.1 kWh/m^2. Implementing photovoltaic panels across the entire area does not significantly reduce energy consumption compared to the baseline.

Adopting cool roofs produces an evident reduction, with consumption lowered to approximately 1.9 kWh/m^2 in the denser areas. Moreover, the lower is λ_p, the lower the energy use per unit surface. Similarly, using 100% green roofs leads to a less pronounced energy reduction than cool roofs, but still better than PVs. In contrast, when urban trees are considered, there is a clear reduction in energy use for space cooling.

When the synergistic effect of the two strategies is examined, the results indicate that combining urban trees with cool roofs produces the most significant energy reduction, with consumption lowered to around 1.0 kWh/m^2 in the core areas. This shows that the combination of reflective materials on roof tops and the shading provided by trees helps significantly reduce cooling energy consumption. This trend can also be identified in the scenarios considering green roofs along with urban trees and photovoltaic panels with urban trees, with the former slightly less effective than the cool roofs with urban trees.

To quantify the reduction in cooling energy use delivered by each strategy, we examine the percentage decrease in energy consumption relative to the baseline scenario, as illustrated in Fig. 10. This analysis reveals that urban trees are the most effective single approach, reducing energy consumption by approximately 46%. Among combined strategies, the most impactful combination is cool roofs and urban trees, which together lower energy consumption by over 50%. An additional noteworthy effect emerges from the combination of photovoltaic panels and urban trees. While slightly less effective than cool roofs and trees, this approach still reduces energy use by around 50%, outperforming urban trees alone. This demonstrates the synergistic benefits of integrating vegetation and renewable energy technologies into urban design.

Finally, to better understand the temporal dynamics of energy consumption, AC energy use was analyzed during three distinct periods: pre-heat wave (July 24–25), heat wave (August 3–4), and post-heat wave (August 8–9). Results indicate a significant

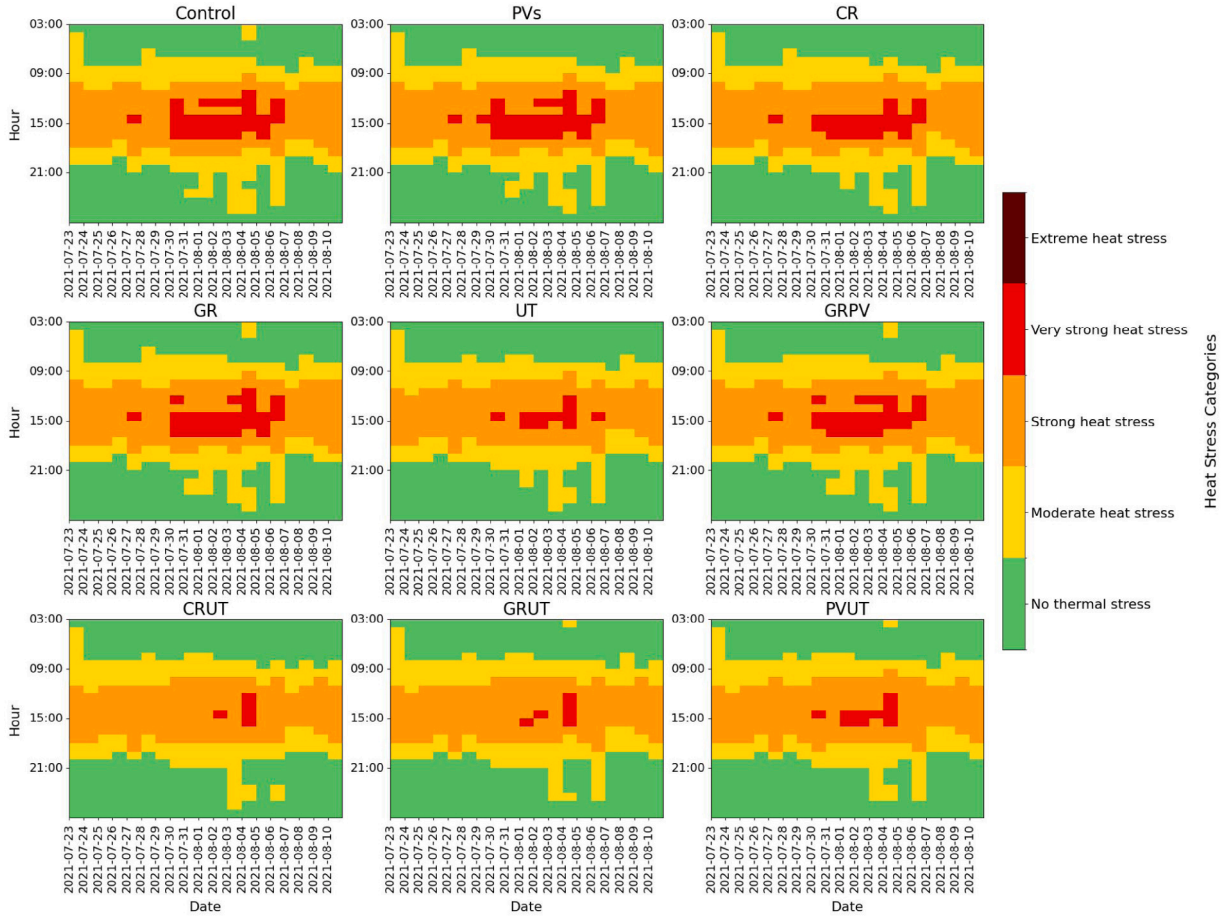

Fig. 7. Heatmap of UTCI 50th percentile showing the hourly distribution of heat stress categories across each day of the simulation period. Top left panel shows the control scenario.

increase in energy consumption during the heatwave period compared to the pre- and post-heatwave periods across all scenarios. For instance, in the baseline scenario, the AC energy consumption increased to 21.32 kWh during the heatwave, contrasting with 15.22 kWh and 14.94 kWh in the pre- and post-heatwave periods, respectively. This pattern of heightened energy consumption during the heatwave, followed by a decline toward pre-heatwave levels, was observed across all the scenarios examined. For example, the energy consumption during the heat wave was 11.07 kWh for the CRUT scenario and 20.60 kWh for the ACPV during the heatwave, while post-heatwave values fell to 6.15 kWh and 14.39 kWh, respectively. The scenarios incorporating combined mitigation approaches, such as cool roofs and urban trees (e.g., CRUT, GRUT, PVUT), used the least energy across all periods. The CRUT scenario achieved the most favorable energy consumption, with values of 6.84 kWh pre-heatwave, 11.07 kWh during the heatwave, and 6.15 kWh post-heatwave. Compared to the baseline and other individual strategies, these findings underscore the effectiveness of combined mitigation strategies in reducing cooling energy demands, even during extreme heat events.

This underscores the profound impact of temperature extremes on AC energy demand, emphasizing the importance of developing adaptive cooling strategies to mitigate peak loads during heat waves.

To estimate the energy produced by photovoltaic panels and determine if it could offset cooling energy consumption, we calculated the difference between the AC energy use for the three scenarios involving PVs and the energy generated by the PVs. The results indicate that the energy generated by the PV systems fully covers the cooling energy consumption in the dense core areas, leading to a net positive energy balance in those zones. As mentioned in Section 2.4, the analysis considered a PV efficiency of 19% and the complete coverage of the building roofs. Furthermore, Fig. 11 demonstrates that while the PV systems maintain a positive energy balance across all investigated scenarios, combining PV panels and urban trees proves to be the most effective. Specifically, in some locations within the densest part of the city, the total net energy available reaches approximately 2.5 kWh/m^2.

As for the 2m air temperature and outdoor heat stress, we investigated the effect of the building's morphology on AC energy use. The bins for λ_p and H are the same considered for the 2m air temperature. In contrast, we consider the percentage reduction between the control run and the different interventions for AC energy use.

Fig. 12 shows the results of this analysis. In the same way as presented for 2m air temperature, the first row of the plot shows rooftop-only strategies, while the second considers urban trees and the combined strategies.

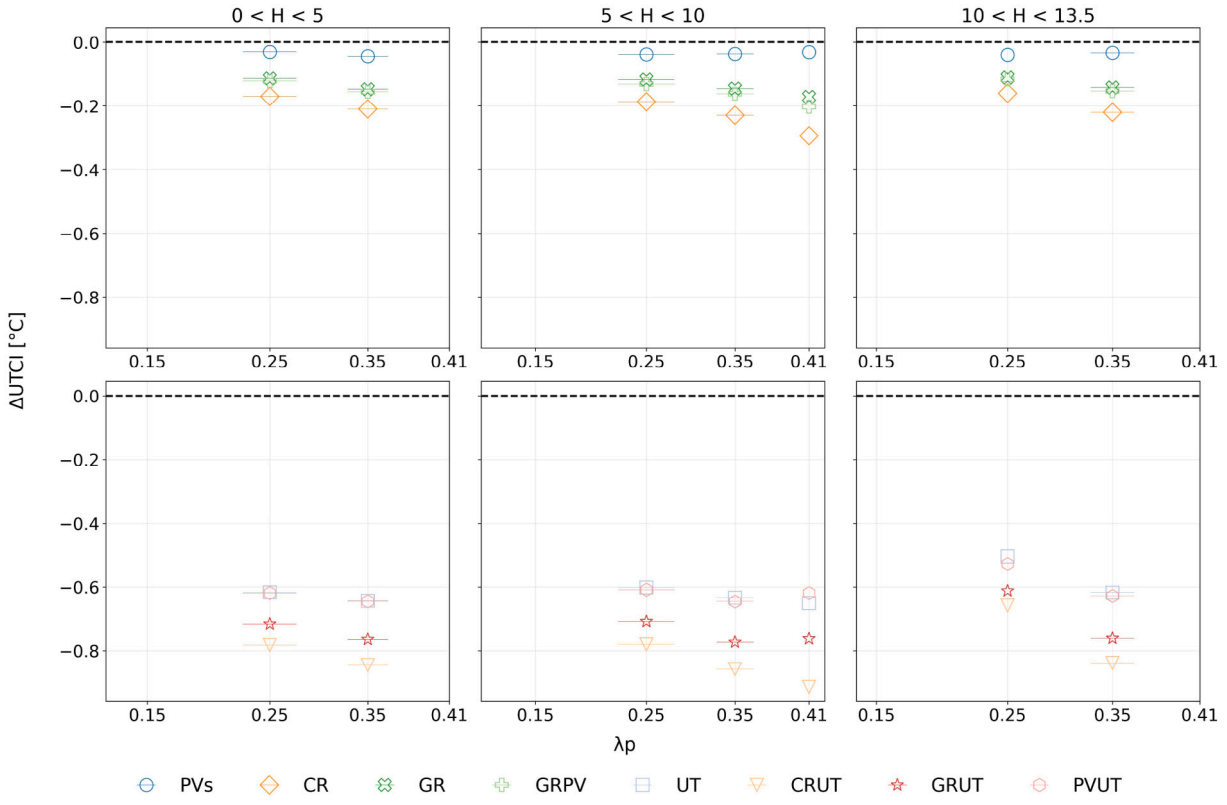

Fig. 8. Reduction of UTCI 50th percentile between each intervention and control run depending on λ_p and building height (H). Building height is constant along the columns, while the rows refer to the strategies. The first row shows rooftop strategies; urban trees are considered in the second.

Photovoltaic panels can moderately reduce cooling energy consumption, typically by 10%–20%, primarily by blocking a portion of direct solar radiation. However, the energy generated by the PV systems has not been considered in the energy use calculations, and the observed reduction in air conditioning energy demand is solely attributable to the shading effect of the PV panels on the building roofs. This PV-based strategy is limited in lowering cooling demand, especially compared to strategies incorporating natural elements such as urban trees or green roofs.

Cool roof surfaces mitigate heat absorption through their high solar reflectance and thermal emissivity, yielding up to 15% cooling energy savings. While effective in lowering rooftop surface temperatures, cool roofs exhibit a limited influence on ambient air temperatures and tend to be less effective in taller building contexts. In contrast to photovoltaic systems, cool roofs directly reduce cooling demands through increased surface albedo but do not match the benefits provided by green-based strategies.

Green roofs, both standalone and in combination with photovoltaic panels, produce almost the same result in every city configuration. For less dense areas characterized by medium-low building heights, the air conditioning energy use reduction is approximately 10%. In contrast, the reduction increases slightly up to 12% for the densest areas. When the buildings are taller, the two strategies become less effective, with the reduction in air conditioning use only around 5%–6%. Compared to PVs and cool roofs, both standalone and combined with photovoltaic panels, green roofs exhibit intermediate performance, performing better than PVs but not as effectively as cool roofs.

Urban trees provide cooling through shading and evapotranspiration, making them a more effective cooling solution than rooftop-based strategies. However, the performance of this approach is influenced by the urban context. As the density of buildings increases, the cooling effectiveness of urban trees decreases, with energy use reductions dropping to around 30%. Similarly, taller building heights also diminish the cooling impact of trees, further reducing energy use savings. This can be attributed to the reduced space available for trees as building density rises and the decreased shading effect when buildings exceed the height of the trees, exposing them to more direct solar radiation and increasing the energy demands for space cooling.

Combining cool roofs and urban trees significantly enhances both strategies' effectiveness, resulting in up to 60% of energy reductions. Trees provide cooling through shading and evapotranspiration, while cool roofs reduce rooftop heating. However, the overall effectiveness of this strategy may be diminished in taller buildings, where shading from trees is less impactful.

Integrating green roofs and urban trees reduces energy use slightly less than the combination of cool roofs and urban trees. The most substantial impact can be found for low buildings and medium-density city configurations, with an approximately 55% reduction in air conditioning energy use. However, when the buildings' height increases, as already seen for the other strategies,

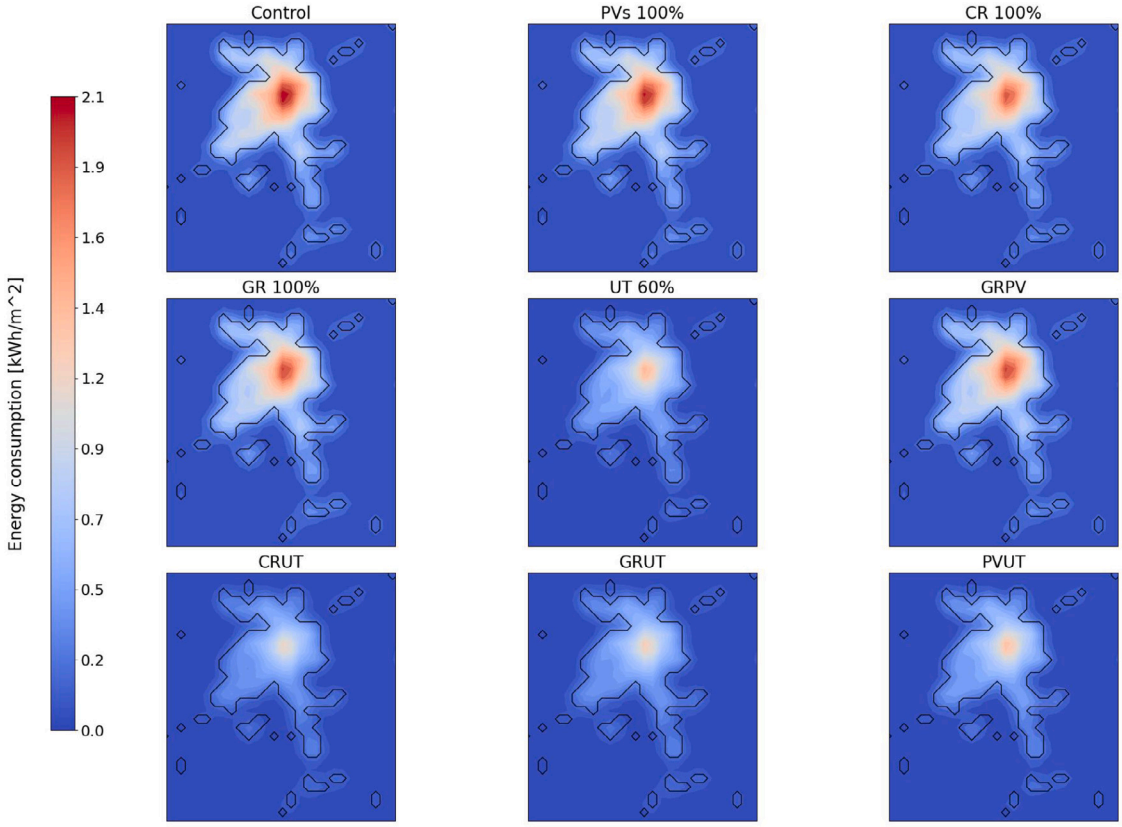

Fig. 9. Total AC energy use [kWh/m^2] for the 19 days for the control run and each strategy. Note that for the scenarios that include PVs the energy generated has not been considered.

AC energy use reduction decreases to approximately 45% for the city's densest area with buildings' height between 5 and 10 m. The smallest reduction is found for buildings' heights between 10 and 13.5 m. For this urban configuration, the energy reduction is around 20% for less dense areas and approximately 40% for denser areas.

Finally, photovoltaic panels combined with urban trees perform better than urban trees alone but worse than cool roofs and green roofs combined with urban trees.

4. Discussion

4.1. Adaptation strategies and 2m air temperature - AC energy use interactions

Our findings highlight the significant potential of integrating cool roofs, green roofs, and urban trees in urban planning as a means to reduce 2m air temperatures and energy consumption. As illustrated in Fig. 4, combining these adaptation strategies produces more pronounced cooling effects, demonstrating their capacity to mitigate urban overheating effectively. Cool roofs, for example, reflect solar radiation, reducing heat gains indoors and thus lowering the demand for air conditioning (AC) use. Similarly, green roofs leverage shading and evapotranspiration, resulting in further cooling benefits and reducing energy needs.

An intriguing aspect of our study is the synergistic relationship between photovoltaic (PV) panels and urban trees. Urban trees provide shading, which reduces cooling loads on buildings, while PV panels, when connected to energy storage systems, generate sufficient energy to meet diurnal cooling demands. This combination maximizes energy savings and reduces urban temperatures, particularly during peak AC demand.

The extent of each strategy's impact, however, can vary depending on specific configurations. For instance, while cool roofs remain the most effective rooftop intervention by reflecting solar radiation, green roofs provide slightly less cooling due to their lower albedo. However, integrating PV panels with green roofs enhances overall cooling performance by leveraging additional shading and evapotranspiration. Urban trees, particularly when paired with rooftop interventions, significantly reduce energy use as well.

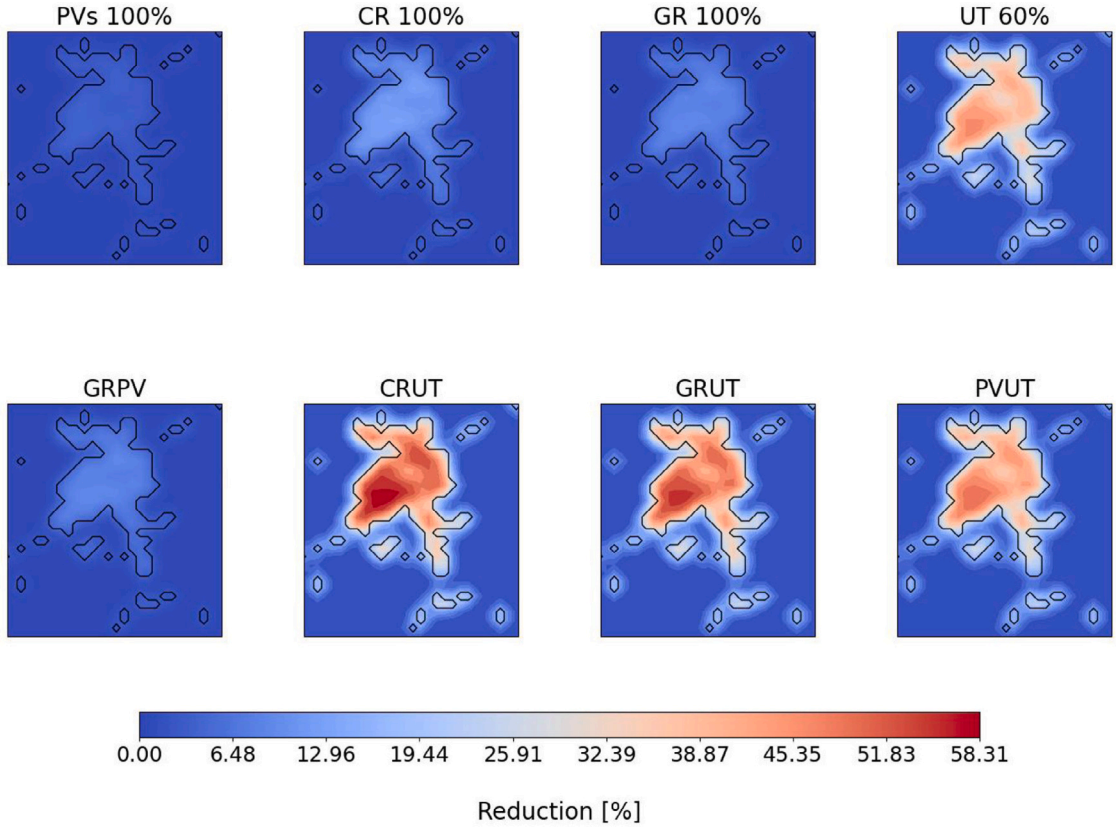

Fig. 10. Percentage reduction of total AC energy use for each strategy for the 19 days. The reduction has been calculated as $((Control - Strategy)/Control) * 100$.

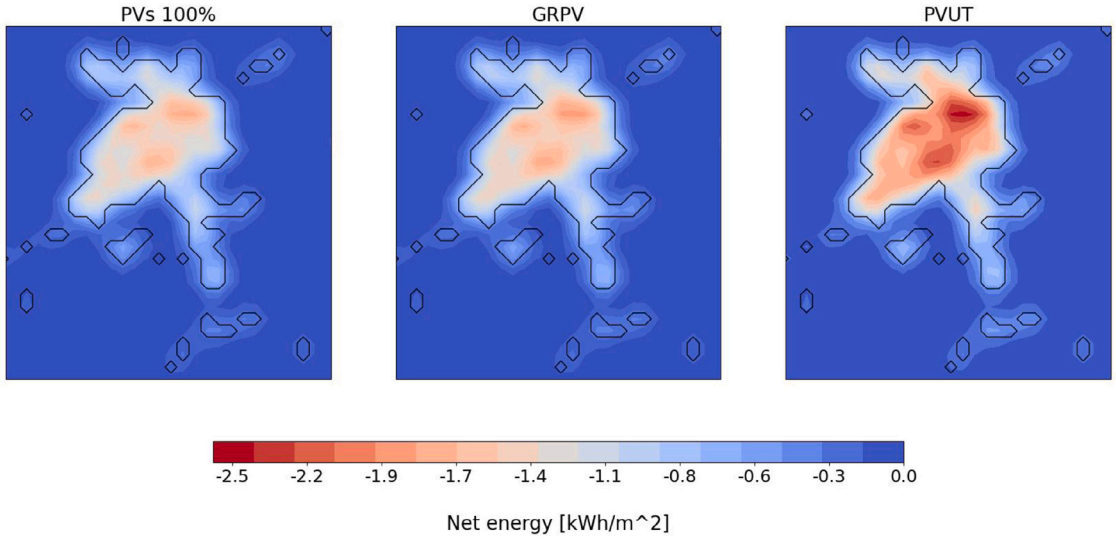

Fig. 11. Total net energy available for the three interventions that implement PVs. The net energy has been calculated as AC energy use — Energy produced by PVs.

Interestingly, Fig. 13 shows that temperature reductions are almost negligible across simulations, revealing a critical disconnect between ambient air temperatures and AC energy use. It is feasible to reduce the energy required for space cooling without necessarily lowering 2m air temperatures. The shading from trees, for instance, maintains cooler building surfaces, which subsequently reduces indoor temperatures and, therefore, the demand for artificial cooling.

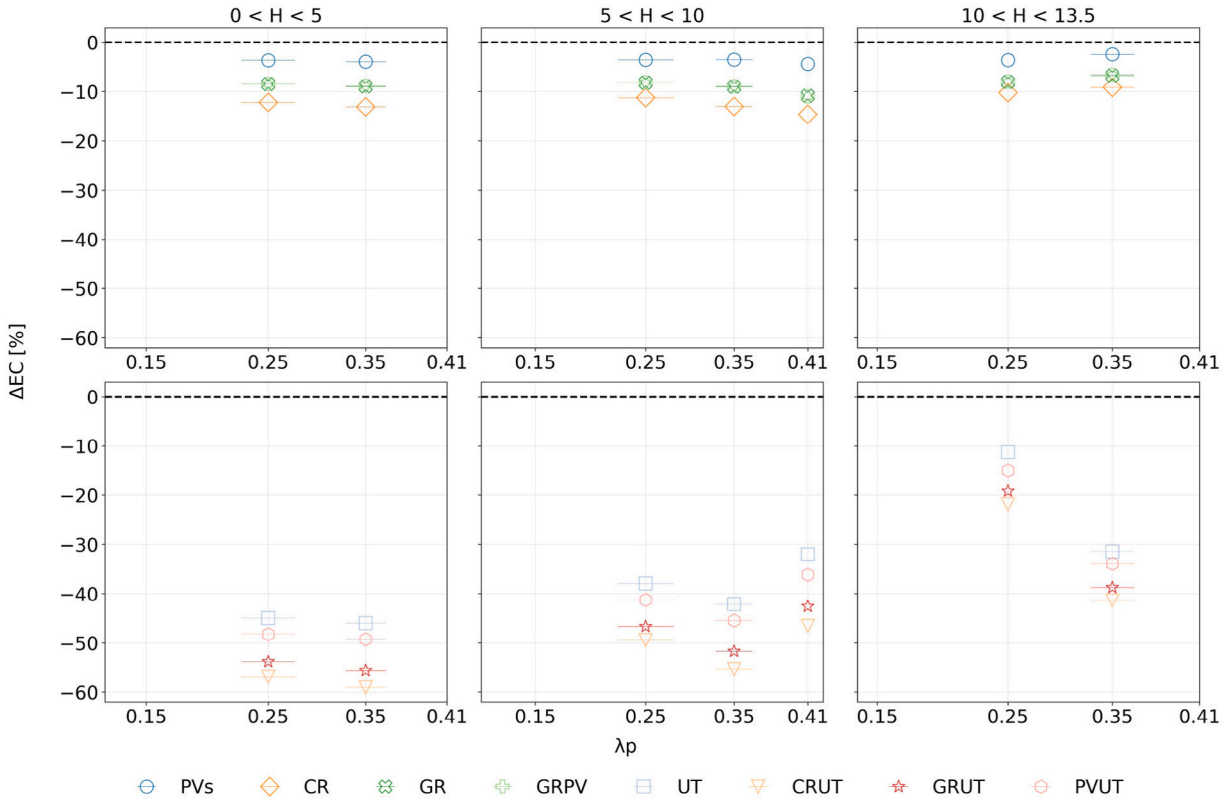

Fig. 12. Total AC energy use percentage reduction between each intervention and control run depending on λ_p and building height (H). Building height is constant along the columns, while the rows refer to the strategies. The first shows rooftop strategies; urban trees are considered in the second.

These findings align well with recent studies that have documented the cooling potential of such adaptation strategies in urban environments. Previous research has shown that cool roofs can decrease air temperatures by up to 2 °C in areas with intense solar exposure, especially during the daytime when AC demand is highest (Wong et al., 2021). Green roofs have similarly demonstrated their ability to lower air temperatures by approximately 1.5 °C while also reducing the need for AC due to their insulating properties (Park et al., 2018). At the street level, trees contribute additional cooling through shade and evapotranspiration, reducing air temperatures by as much as 2–3 °C and mitigating the urban heat island effect (Johnson and Breil, 2012; Feyisa et al., 2014). These studies underscore the role of green infrastructure and cool surfaces as effective measures for reducing urban heat stress and improving energy efficiency, aligning closely with the synergistic strategies highlighted in our study.

4.2. Adaptation strategies and outdoor heat stress - AC energy use interactions

Our analysis shows that, beyond reducing 2m air temperatures, these interventions have a significant impact on outdoor heat stress at the pedestrian level. The results, particularly noticeable during daytime, indicate that urban trees play a critical role in reducing pedestrian heat stress (Fig. 7). This reduction is primarily driven by the shade provided by trees, which reduces direct solar exposure and lowers longwave radiation emitted from shaded urban surfaces. When urban trees are combined with other strategies, such as cool roofs, the reduction in heat stress becomes even more pronounced and extends into nighttime hours. As with 2m air temperature reductions, the effect's magnitude is location-specific, largely influenced by surrounding building geometry and usage patterns.

In examining the relationship between 2m air temperature, outdoor heat stress, and AC energy use, we focused on three UTCI percentiles—10th, 50th, and 90th—to represent cool spots, average conditions, and hot spots. Our analysis of these adaptation strategies' impact reveals substantial reductions in AC energy consumption, with urban trees proving to be the most effective intervention in mitigating heat stress. Specifically, urban trees consistently reduced heat stress-degree hours by 20 to 25 h, compared to the 5-hour reduction achieved by cool roofs and green roofs across all three UTCI percentiles (Fig. 14). This cooling effect extended well beyond individual grid cells, lowering heat stress-degree hours across the study period, particularly for high-stress UTCI conditions.

When strategies were combined, cool roofs paired with urban trees yielded the most effective reduction in heat stress, followed closely by the combination of green roofs and urban trees. Although the combination of photovoltaic panels and urban trees showed

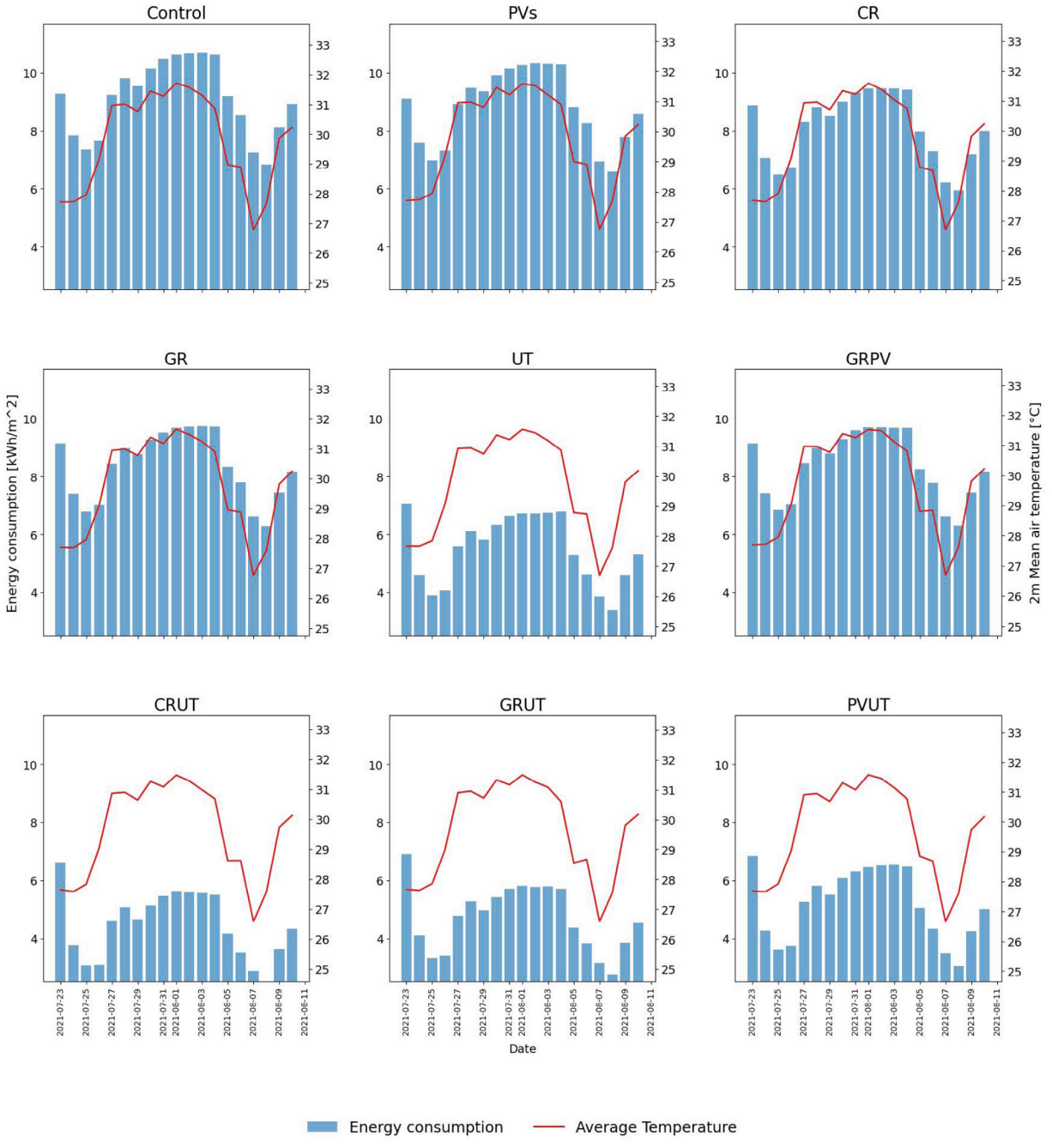

Fig. 13. Effects of strategies on average 2m air temperature and total AC energy use over the 19 days. Top left panel shows the Control run. The PVs energy generated has not been considered.

a smaller reduction in heat stress hours, it provided an added advantage by meeting cooling energy demand through solar energy generation. Based on the IPCC definitions of adaptation and mitigation strategies (Watson et al., 2001), this approach—pairing urban trees with photovoltaic panels—emerges as a comprehensive intervention. The trees reduce outdoor heat stress through shading and cooling. At the same time, the photovoltaic panels generate renewable energy to support air conditioning, distinguishing this approach from other strategies that do not produce energy for cooling.

These findings are in line with other research, which highlights urban tree cover as a primary strategy for improving outdoor thermal comfort. Studies indicate that urban vegetation can reduce air temperatures by 1 to 7 °C compared to nearby urban areas (Zölch et al., 2016; Piselli et al., 2018; Meili et al., 2021; Stone et al., 2023). The substantial cooling impact found in our

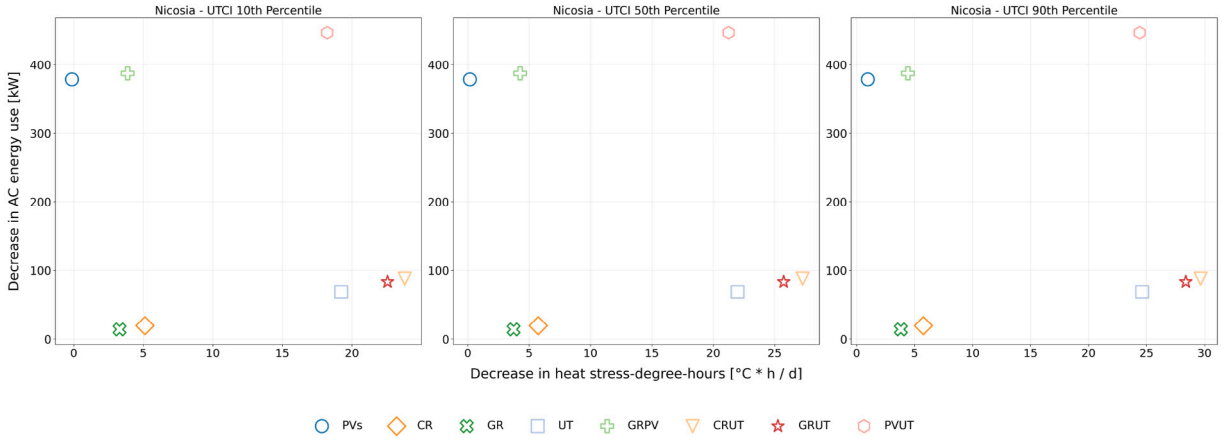

Fig. 14. Effects of strategies on outdoor heat stress and AC energy use based on the three different UTCI percentiles: 10th, 50th, and 90th. The decrease in AC energy use has been determined considering the energy produced by PVs, while for outdoor heat stress the hourly degree-hours exceeding the slight heat stress UTCI threshold of 26 °C have been calculated.

study, especially during daytime, reflects these broader findings and underscores the importance of vegetation in alleviating urban heat stress. The shade provided by trees and the reduced surface radiation contribute to notable improvements in outdoor comfort, supporting the efficacy of green infrastructure as a valuable tool in urban adaptation strategies.

4.3. Adaptation strategies and building geometry

Beyond examining the effect of strategies on 2m air temperature, outdoor heat stress, and AC energy use at the city scale, this study also provides insights into the relationship between the intervention and the city geometry. We focused on two key parameters: building density λ_p and building height H. To account for the heterogeneous layout of buildings within the city, we categorized density and height into distinct bins. The λ_p bins were established at 0.15, 0.25, 0.35, and 0.41, representing different levels of urban density. For building height, we considered three categories: 5, 10, and 13.5 m. This classification allows a more refined analysis on how urban interventions interact with varying city structures.

Across all variable examined, two distinct patterns emerge: one for rooftop interventions and another for urban trees (Figs. 5, 8, and 12). When urban trees are combined with rooftop strategies the resulting effect mirrors that of urban trees alone. Generally, all rooftop strategies contribute to air temperature mitigation, with the most significant reductions occurring in areas with medium-height and higher-density buildings. Photovoltaic panels stand out as the sole rooftop strategy that produces negligible temperature reductions. This differentiation in effectiveness highlights the varying impacts of different urban cooling strategies depending on the built environment characteristics.

In contrast to rooftop strategies, urban trees generate more pronounced temperature reductions. Rooftop strategies exhibit a quasi-linear reduction tendency, while urban trees display a quasi-quadratic trend with a minimum point at $\lambda_p = 0.35$ across all building heights. The strongest reduction is achieved by pairing urban trees with cool roofs in the city configuration characterized by $\lambda_p = 0.35$ and $5 < H < 10$ m. A similar outcome is found for the tallest buildings, whereas the mitigation is less pronounced for the lowest buildings. This may be attributed to the shading provided by the trees and the taller and denser buildings. The mitigation of outdoor heat stress aligns with air temperature trends, showing a more significant effect when considering urban trees alone or combined with rooftop strategies, particularly cool roofs.

Examining AC energy use, cool roofs yield the most substantial decrease among rooftop strategies alone, followed by green roofs and green roofs with photovoltaic panels. Nevertheless, the benefits of rooftop strategies are reduced for taller buildings, and a similar effect is observed for rooftop strategies combined with urban trees. The relationship between building density, height, and AC energy use reaches a minimum point when $\lambda_p = 0.35$ and building heights are between 5 and 10 m, similar to the trend observed for 2m air temperature.

To further explore the topic, it is worth examining the relationship between the AC energy use for space cooling per square meter of floor area and the surface-to-volume ratio (S/V) based on the varying densities across the city. The specific energy consumption is calculated by dividing the total energy consumption by the product of λ_p and the normalized average building height, where the latter is represented by the ratio of average building height to 5 m, the typical story height. This calculation indicates energy use efficiency based on the total floor area rather than solely the building footprint.

The analysis revealed some notable patterns in Nicosia's energy consumption. Fig. 15 shows that specific energy consumption decreases as building density increases. For instance, energy consumption is the lowest for buildings between 5 and 10 m, and λ_p= 0.41 following the idea that more compact cities typically exhibit smaller surface-to-volume ratios and lower potential for heat gains (Martilli, 2014). However, Fig. 16 shows that for buildings with a height between 10 and 15 m, specific energy consumption rises significantly as urban density increases. This cannot be attributed solely to the diminished ventilation and natural cooling

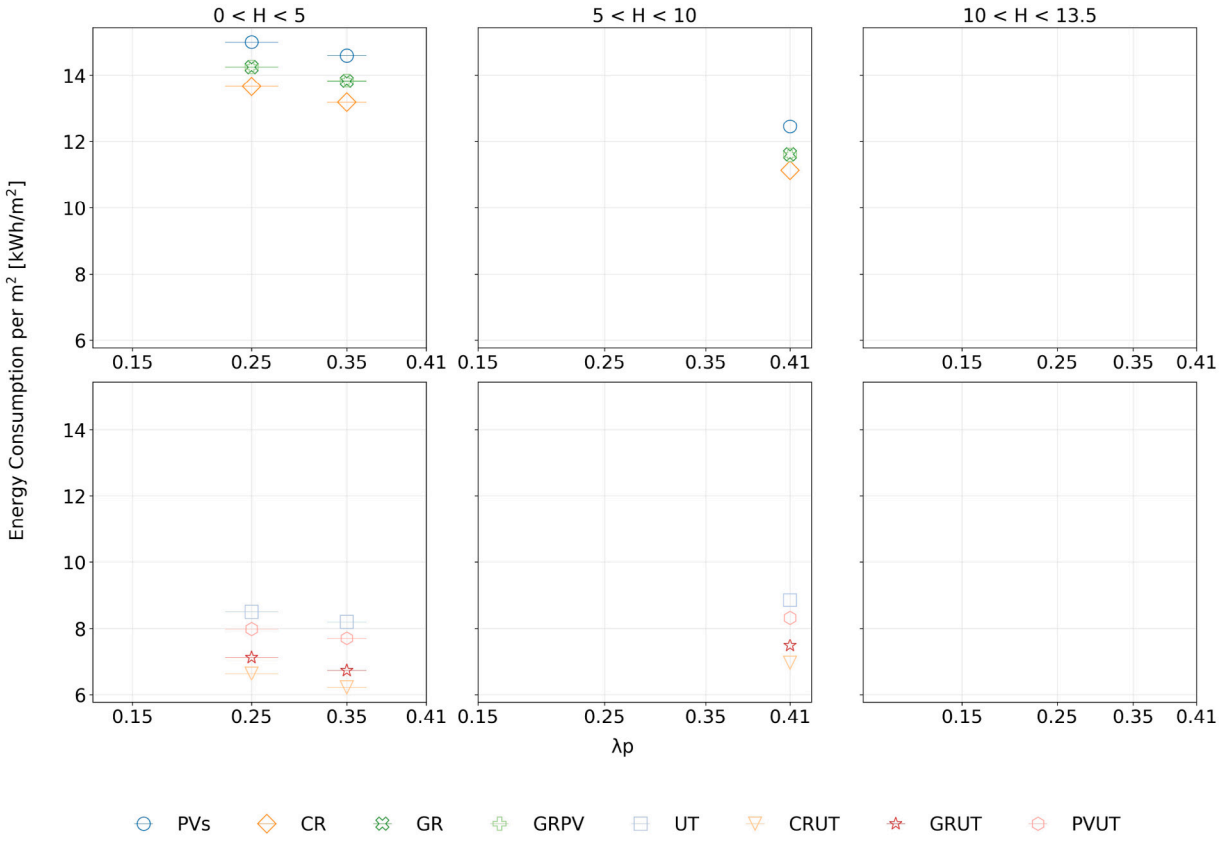

Fig. 15. Energy consumption per square meter of floor area for all urban areas within Nicosia's boundaries without considering the old town, according to different buildings density λ_p and height H.

capabilities in denser areas or the urban heat island effect but also to the varying construction materials used in this part of the city. Despite having a more favorable surface-to-volume ratio, older buildings are sensibly less energy-efficient. As a result, they require more energy to maintain comfortable indoor conditions, or they experience higher indoor temperatures without air conditioning. This would explain why the higher energy consumption appears in the city's old town, where buildings are characterized by lower-performing materials compared to the rest of the city, as mentioned in Section 2.3.3.

The analyses underscore a nuanced understanding that refutes the simplistic notion that increasing urban tree cover is inherently beneficial. Instead, it highlights the complex interplay of factors, including the specific functions and built environment characteristics of different urban settings, which influence the efficacy of cooling interventions. Further investigation is necessary to identify these underlying elements, as this knowledge could inform the development of tailored, optimal configurations suited to the unique attributes of diverse urban environments, ultimately enabling more targeted and efficient urban cooling strategies.

5. Conclusions

As cities face escalating challenges from overheating, particularly in regions identified as climate change hotspots, such as the Eastern Mediterranean and Middle East, the need for effective adaptation strategies is becoming increasingly urgent. To enhance resilience against the intensifying impacts of extreme heat, municipalities are exploring various infrastructure-based adaptation strategies, such as street trees, rooftop photovoltaic systems, and cool and green roofs. However, each of these strategies comes with potential benefits and drawbacks. In this study, we employed an urbanized mesoscale atmospheric model to quantify the impacts of these four adaptation strategies and their combination over 19 summer days in Nicosia, assessing their effects on 2m air temperature, outdoor thermal stress, and space cooling energy use. The key findings are summarized below:

1. All examined adaptation strategies (cool roofs, green roofs, urban trees, photovoltaic panels) impact the outcomes of air temperature, outdoor thermal comfort, and energy use and involve trade-offs. The results also suggest that underlying factors, such as the diverse functions of specific urban areas, warrant further investigation. Identifying these factors could enable the development of optimal strategy configurations tailored to the unique characteristics of different urban environments, ultimately enhancing their resilience to climate change challenges.

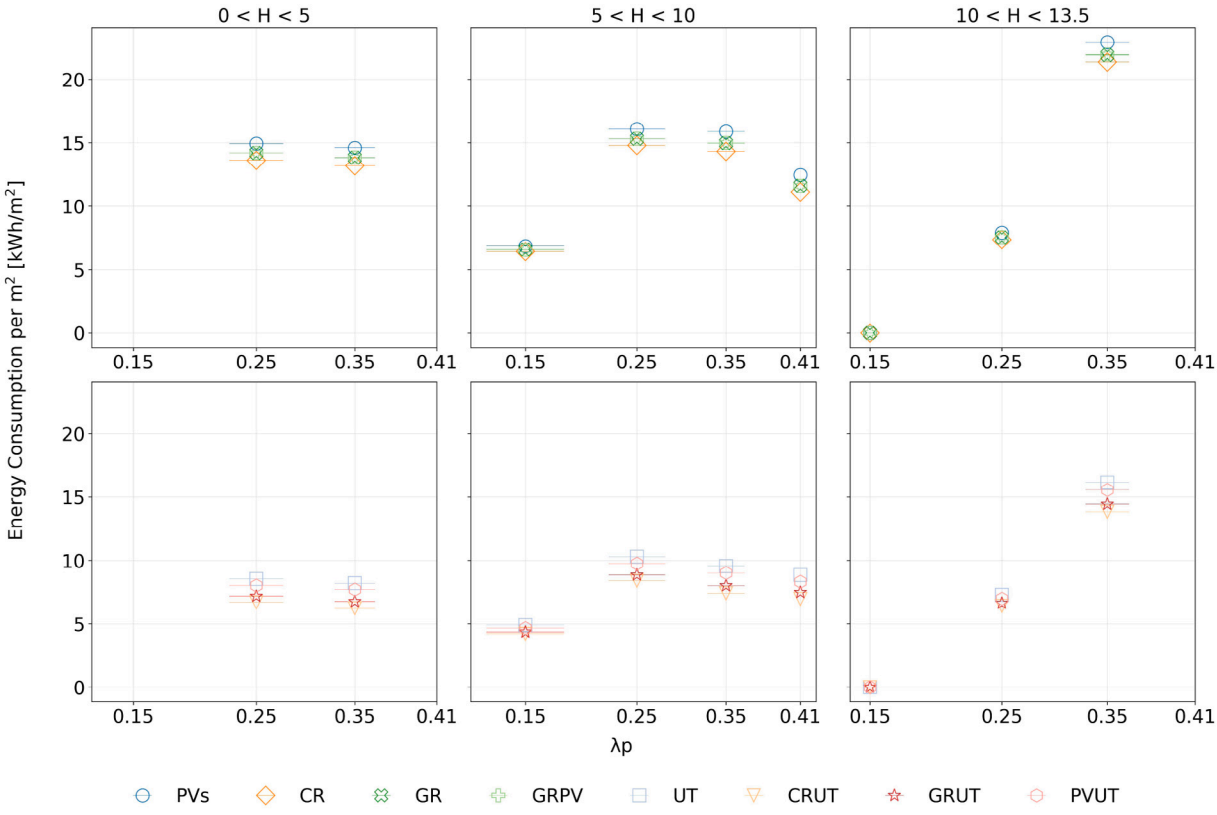

Fig. 16. Energy consumption per square meter of floor area for all urban areas within Nicosia's boundaries, according to different buildings density λ_p and height H.

2. Substantial urban tree cover is more effective than rooftop strategies alone in mitigating daytime outdoor heat stress. The decrease in temperature and mean radiant temperature outweighs any minor increase in UTCI from higher relative humidity from transpiration, especially in semi-arid climates like Nicosia.
3. Extensive tree cover can also reduce energy use for space cooling.
4. PVs are the least efficient rooftop strategy for reducing air temperature and outdoor heat stress. However, given adequate electrical or thermal storage, comprehensive PV roof coverage could potentially generate enough energy to satisfy the city center's diurnal air conditioning needs during a typical summer.
5. Cool roofs are more effective than green roofs in reducing heat stress, lowering 2m air temperature, and decreasing energy use for space cooling. Additionally, studies have suggested that street trees should preferably be planted on the north side of streets to maximize reductions in heat exposure (Zhao et al., 2018; Lachapelle et al., 2023). Furthermore, attention should be paid to the planting configuration to minimize impacts on pollutant ventilation (Vos et al., 2013).
6. An intricate relationship exists between adaptation strategies, their outcomes, and the city's configuration and geometry. Varying the urban geometry can significantly impact the performance of certain strategies. This suggests that defining optimal strategy configurations requires considering the unique characteristics of different urban environments. Ultimately, the optimal implementation of heat adaptation strategies must be tailored to the specific location.

In summary, the study highlights two key strategies for urban climate adaptation and mitigation:

- Combining urban trees with cool roofs offers the most effective heat mitigation across the multiple dimensions evaluated in this research.
- Combining street trees with photovoltaic panels is a promising strategy due to the energy generation capabilities of PVs, which can power cooling systems along with trees' cooling effect, thereby enhancing the resilience of the thermal environment during heat waves, making them crucial to a comprehensive climate change strategy. However, their heat stress reduction is less pronounced than urban trees and cool roofs.

Overall, this study offers a comprehensive analysis that extends beyond typical evaluations focused solely on temperature reduction. A more holistic understanding of their effects is achieved by assessing the dual impacts of adaptation and mitigation strategies on thermal comfort and energy use. The novel incorporation of high-resolution urban data, coupled with examining

outcomes across varying urban densities, yields insights into the localized implications of these strategies. While the feasibility of some approaches may face practical or economic constraints, the findings nonetheless offer valuable guidance to policymakers tasked with developing tailored climate resilience measures for semi-arid environments. By addressing heat stress and energy consumption, this work contributes meaningful insights to the growing body of scholarship on urban climate adaptation, particularly within the vulnerable Eastern Mediterranean and Middle East region.

CRediT authorship contribution statement

Giandomenico Vurro: Writing – review & editing, Writing – original draft, Visualization, Software, Methodology, Investigation, Formal analysis, Data curation, Conceptualization. **Alberto Martilli:** Writing – review & editing, Supervision, Software, Methodology, Conceptualization. **Panos Hadjinicolaou:** Writing – review & editing, Supervision, Project administration, Methodology, Funding acquisition, Conceptualization. **Salvatore Carlucci:** Writing – review & editing, Supervision, Conceptualization. **Katiana Constantinidou:** Writing – review & editing, Methodology. **Jos Lelieveld:** Writing – review & editing, Supervision, Funding acquisition, Conceptualization.

Declaration of competing interest

The authors declare that they have no known competing financial interests or personal relationships that could have appeared to influence the work reported in this paper.

Acknowledgments

This work was supported by the EMME-CARE project, which received funding from the European Union's Horizon 2020 Research and Innovation Programme under grant agreement no. 856612, as well as matching co-funding by the Government of the Republic of Cyprus.

Supplementary data

Supplementary material related to this article can be found online at https://doi.org/10.1016/j.uclim.2025.102507.

Data availability

Data will be made available on request.

References

Alexandru, A., de Elia, R., Laprise, R., 2007. Internal variability in regional climate downscaling at the seasonal scale. Mon. Weather Rev. 135 (9), 3221–3238.
Aminipouri, M., Rayner, D., Lindberg, F., Thorsson, S., Knudby, A.J., Zickfeld, K., Middel, A., Krayenhoff, E.S., 2019. Urban tree planting to maintain outdoor thermal comfort under climate change: The case of Vancouver's local climate zones. Build. Environ. 158, 226–236.
ASHRAE, 2017. ASHRAE standard 55: Thermal environmental conditions for human occupancy. American Society of Heating, Refrigerating, and Air-Conditioning Engineers, ANSI/ASHRAE Standard 55-2017, https://www.ashrae.org/technical-resources/standards-and-guidelines.
Bougeault, P., Lacarrere, P., 1989. Parameterization of orography-induced turbulence in a mesobeta–scale model. Mon. Weather Rev. 117 (8), 1872–1890.
Broadbent, A.M., Declet-Barreto, J., Krayenhoff, E.S., Harlan, S.L., Georgescu, M., 2022. Targeted implementation of cool roofs for equitable urban adaptation to extreme heat. Sci. Total Environ. 811, 151326.
Broadbent, A.M., Krayenhoff, E.S., Georgescu, M., 2020. Efficacy of cool roofs at reducing pedestrian-level air temperature during projected 21st century heatwaves in Atlanta, Detroit, and Phoenix (USA). Environ. Res. Lett. 15 (8), 084007.
Brousse, O., Simpson, C.H., Zonato, A., Martilli, A., Taylor, J., Davies, M., Heaviside, C., 2023. Cool roofs could be most effective at reducing outdoor urban temperatures in London compared with other roof top and vegetation interventions: a mesoscale urban climate modelling study. Authorea Preprint.
Cartalis, C., Synodinou, A., Proedrou, M., Tsangrassoulis, A., Santamouris, M., 2001. Modifications in energy demand in urban areas as a result of climate changes: an assessment for the southeast Mediterranean region. Energy Convers. Manage. 42 (14), 1647–1656.
Castaño-Rosa, R., Barrella, R., Sánchez-Guevara, C., Barbosa, R., Kyprianou, I., Paschalidou, E., Thomaidis, N.S., Dokupilova, D., Gouveia, J.P., Kádár, J., et al., 2021. Cooling degree models and future energy demand in the residential sector. A seven-country case study. Sustainability 13 (5), 2987.
Chen, F., Dudhia, J., 2001. Coupling an advanced land surface–hydrology model with the Penn State–NCAR MM5 modeling system. Part I: Model implementation and sensitivity. Mon. Weather Rev. 129 (4), 569–585.
Chen, F., Kusaka, H., Bornstein, R., Ching, J., Grimmond, C., Grossman-Clarke, S., Loridan, T., Manning, K.W., Martilli, A., Miao, S., et al., 2011. The integrated WRF/urban modelling system: development, evaluation, and applications to urban environmental problems. Int. J. Climatol. 31 (2), 273–288.
Cramer, W., Guiot, J., Fader, M., Garrabou, J., Gattuso, J.-P., Iglesias, A., Lange, M.A., Lionello, P., Llasat, M.C., Paz, S., et al., 2018. Climate change and interconnected risks to sustainable development in the Mediterranean. Nat. Clim. Chang. 8 (11), 972–980.
Fanger, P.O., 1970. Thermal Comfort: Analysis and Applications in Environmental Engineering. McGraw-Hill, New York.
Feyisa, G.L., Dons, K., Meilby, H., 2014. Efficiency of parks in mitigating urban heat island effect: An example from Addis Ababa. Landsc. Urban Plan. 123, 87–95.
Fokaides, P.A., Christoforou, E.A., Kalogirou, S.A., 2014. Legislation driven scenarios based on recent construction advancements towards the achievement of nearly zero energy dwellings in the southern European country of Cyprus. Energy 66, 588–597.
Fung, K.Y., Yang, Z.-L., Martilli, A., Krayenhoff, E.S., Niyogi, D., 2024. Prioritizing social vulnerability in urban heat mitigation. PNAS Nexus 3 (9), pgae360.
Gabeiras, J., 2024. wrfup: A Python package for urban parameter calculation and integration into WRF models. URL https://github.com/jacobogabeiraspenas/wrfup. (Accessed 15 May 2024).

Geletič, J., Lehnert, M., Resler, J., Krč, P., Middel, A., Krayenhoff, E., Krüger, E., 2022. High-fidelity simulation of the effects of street trees, green roofs and green walls on the distribution of thermal exposure in Prague-Dejvice. Build. Environ. 223, 109484.
Georgescu, M., Morefield, P.E., Bierwagen, B.G., Weaver, C.P., 2014. Urban adaptation can roll back warming of emerging megapolitan regions. Proc. Natl. Acad. Sci. 111 (8), 2909–2914.
Giorgi, F., 2006. Climate change hot-spots. Geophys. Res. Lett. 33 (8).
Giorgi, F., Bi, X., 2000. A study of internal variability of a regional climate model. J. Geophys. Res.: Atmospheres 105 (D24), 29503–29521.
Hadjinicolaou, P., Giannakopoulos, C., Zerefos, C., Lange, M.A., Pashiardis, S., Lelieveld, J., 2011. Mid-21st century climate and weather extremes in Cyprus as projected by six regional climate models. Reg. Environ. Chang. 11, 441–457.
Hadjinicolaou, P., Tzyrkalli, A., Zittis, G., Lelieveld, J., 2023. Urbanisation and geographical signatures in observed air temperature station trends over the Mediterranean and the Middle East–North Africa. Earth Syst. Environ. 7, 649–659. http://dx.doi.org/10.1007/s41748-023-00348-y.
Heaviside, C., Vardoulakis, S., Cai, X.-M., 2016. Attribution of mortality to the urban heat island during heatwaves in the West Midlands, UK. Environ. Heal. 15, 49–59.
Hersbach, H., Bell, B., Berrisford, P., Hirahara, S., Horányi, A., Muñoz-Sabater, J., Nicolas, J., Peubey, C., Radu, R., Schepers, D., et al., 2020. The ERA5 global reanalysis. Q. J. R. Meteorol. Soc. 146 (730), 1999–2049.
Hong, S.-Y., Lim, J.-O.J., 2006. The WRF single-moment 6-class microphysics scheme (WSM6). Asia- Pac. J. Atmospheric Sci. 42 (2), 129–151.
Iacono, M.J., Delamere, J.S., Mlawer, E.J., Shephard, M.W., Clough, S.A., Collins, W.D., 2008. Radiative forcing by long-lived greenhouse gases: Calculations with the AER radiative transfer models. J. Geophys. Res.: Atmospheres 113 (D13).
ISO7730, 2005. ISO 7730:2005 - Ergonomics of the thermal environment – Analytical determination and interpretation of thermal comfort using calculation of the PMV and PPD indices and local thermal comfort criteria. International Organization for Standardization, ISO 7730:2005 URL https://www.iso.org/standard/39155.html.
Iungman, T., Cirach, M., Marando, F., Barboza, E.P., Khomenko, S., Masselot, P., Quijal-Zamorano, M., Mueller, N., Gasparrini, A., Urquiza, J., et al., 2023. Cooling cities through urban green infrastructure: a health impact assessment of European cities. Lancet 401 (10376), 577–589.
Jiang, T., Krayenhoff, E.S., Martilli, A., Nazarian, N., Stone, B., Voogt, J.A., 2025. Prioritizing urban heat adaptation infrastructure based on multiple outcomes: comfort, health, and energy. Proceed. National Academy Sci. 122 (19), e2411144122. http://dx.doi.org/10.1073/pnas.2411144122.
Johnson, K., Breil, M., 2012. Conceptualizing urban adaptation to climate change-findings from an applied adaptation assessment framework. FEEM Working Paper.
Kain, J.S., 2004. The Kain–Fritsch convective parameterization: an update. J. Appl. Meteorol. 43 (1), 170–181.
Kekkou, F., Lazoglou, G., Economou, T., Anagnostopoulou, C., 2023. Exploring the association of heat stress and human health in Cyprus. Environ. Sci. Proc. 26 (1), http://dx.doi.org/10.3390/environsciproc2023026084, URL https://www.mdpi.com/2673-4931/26/1/84.
Kolokotsa, D., Santamouris, M., Zerefos, S., 2013. Green and cool roofs' urban heat island mitigation potential in European climates for office buildings under free floating conditions. Sol. Energy 95, 118–130.
Köppen, W., 1884. Die wärmezonen der erde, nach der dauer der heissen, gemässigten und kalten zeit und nach der wirkung der wärme auf die organische welt betrachtet. publisher not identified.
Kottek, M., Grieser, J., Beck, C., Rudolf, B., Rubel, F., 2006. World map of the Köppen-Geiger climate classification updated.
Krayenhoff, E.S., Moustaoui, M., Broadbent, A.M., Gupta, V., Georgescu, M., 2018. Diurnal interaction between urban expansion, climate change and adaptation in US cities. Nat. Clim. Chang. 8 (12), 1097–1103.
Kulmala, M., Nieminen, T., Chellapermal, R., Makkonen, R., Bäck, J., Kerminen, V.-M., 2013. Climate feedbacks linking the increasing atmospheric CO 2 concentration, BVOC emissions, aerosols and clouds in forest ecosystems. Biology, Control. Model. Tree Volatile Org. Compd. Emiss. 489–508.
Lachapelle, J.A., Krayenhoff, E.S., Middel, A., Coseo, P., Warland, J., 2023. Maximizing the pedestrian radiative cooling benefit per street tree. Landsc. Urban Plan. 230, 104608.
Lavin-Gullon, A., Fernandez, J., Bastin, S., Cardoso, R.M., Fita, L., Giannaros, T.M., Goergen, K., Gutiérrez, J.M., Kartsios, S., Katragkou, E., et al., 2021. Internal variability versus multi-physics uncertainty in a regional climate model. Int. J. Climatol. 41 (S1), E656–E671.
Lazoglou, G., Hadjinicolaou, P., Sofokleous, I., Bruggeman, A., Zittis, G., 2024. Climate change and extremes in the Mediterranean island of Cyprus: from historical trends to future projections. Environ. Res. Commun. 6 (9), 095020. http://dx.doi.org/10.1088/2515-7620/ad7927.
Lee, H., Mayer, H., Chen, L., 2016. Contribution of trees and grasslands to the mitigation of human heat stress in a residential district of Freiburg, Southwest Germany. Landsc. Urban Plan. 148, 37–50.
Lelieveld, J., Hadjinicolaou, P., Kostopoulou, E., Chenoweth, J., El Maayar, M., Giannakopoulos, C., Hannides, C., Lange, M., Tanarhte, M., Tyrlis, E., et al., 2012. Climate change and impacts in the Eastern Mediterranean and the Middle East. Clim. Change 114, 667–687.
Li, D., Bou-Zeid, E., Oppenheimer, M., 2014. The effectiveness of cool and green roofs as urban heat island mitigation strategies. Environ. Res. Lett. 9 (5), 055002.
Lubczyńska, M.J., Christophi, C.A., Lelieveld, J., 2015. Heat-related cardiovascular mortality risk in Cyprus: a case-crossover study using a distributed lag non-linear model. Environ. Heal. 14, 1–11.
Ma, S., Goldstein, M., Pitman, A., Haghdadi, N., MacGill, I., 2017. Pricing the urban cooling benefits of solar panel deployment in Sydney, Australia. Sci. Rep. 7 (1), 43938.
Macintyre, H., Heaviside, C., 2019. Potential benefits of cool roofs in reducing heat-related mortality during heatwaves in a European city. Environ. Int. 127, 430–441.
Marconcini, M., Esch, T., Metz, A., et al., 2021. World Settlement Footprint 3D - A first three-dimensional survey of the global building stock. ResearchGate, URL https://www.researchgate.net/publication/357678737_World_Settlement_Footprint_3D_-_A_first_three-dimensional_survey_of_the_global_building_stock.
Martilli, A., 2014. An idealized study of city structure, urban climate, energy consumption, and air quality. Urban Clim. 10, 430–446.
Martilli, A., Clappier, A., Rotach, M.W., 2002. An urban surface exchange parameterisation for mesoscale models. Bound.-Layer Meteorol. 104 (2), 261–304.
Martilli, A., Nazarian, N., Krayenhoff, E.S., Lachapelle, J., Lu, J., Rivas, E., Rodriguez-Sanchez, A., Sanchez, B., Santiago, J.L., 2023. WRF-Comfort: Simulating micro-scale variability of outdoor heat stress at the city scale with a mesoscale model. EGUsphere 2023, 1–30.
Martilli, A., Nazarian, N., Krayenhoff, E.S., Lachapelle, J., Lu, J., Rivas, E., Rodriguez-Sanchez, A., Sanchez, B., Santiago, J.L., 2024. WRF-Comfort: simulating microscale variability in outdoor heat stress at the city scale with a mesoscale model. Geosci. Model. Dev. 17 (12), 5023–5039.
Meili, N., Acero, J.A., Peleg, N., Manoli, G., Burlando, P., Fatichi, S., 2021. Vegetation cover and plant-trait effects on outdoor thermal comfort in a tropical city. Build. Environ. 195, 107733.
Microsoft, 2024. Microsoft global building footprints. URL https://github.com/microsoft/GlobalMLBuildingFootprints. (Accessed 10 April 2024).
Oke, T.R., 1988. Street design and urban canopy layer climate. Energy Build. 11 (1–3), 103–113.
Oke, T.R., Mills, G., Christen, A., Voogt, J.A., 2017. Urban Climates. Cambridge University Press.
Park, J., Kim, J.-H., Dvorak, B., Lee, D.K., 2018. The role of green roofs on microclimate mitigation effect to local climates in summer. Int. J. Environ. Res. 12, 671–679.
Patel, P., Roth, M., 2022. A High-Resolution Dataset of Global Urban Fraction for Mesoscale Urban Modelling. Zenodo, http://dx.doi.org/10.5281/zenodo.6994975.
Peel, M.C., Finlayson, B.L., McMahon, T.A., 2007. Updated world map of the Köppen-Geiger climate classification. Hydrol. Earth Syst. Sci. 11 (5), 1633–1644.
Petrovic, D., Fersch, B., Kunstmann, H., 2024. Heat wave characteristics: evaluation of regional climate model performances for Germany. Nat. Hazards Earth Syst. Sci. 24 (1), 265–289.

Piselli, C., Castaldo, V., Pigliautile, I., Pisello, A., Cotana, F., 2018. Outdoor comfort conditions in urban areas: On citizens' perspective about microclimate mitigation of urban transit areas. Sustain. Cities Soc. 39, 16–36.
Piselli, C., Pisello, A.L., Saffari, M., de Gracia, A., Cotana, F., Cabeza, L.F., 2019. Cool roof impact on building energy need: The role of thermal insulation with varying climate conditions. Energies 12 (17), 3354.
Pyrgou, A., Hadjinicolaou, P., Santamouris, M., 2020. Urban-rural moisture contrast: Regulator of the urban heat island and heatwaves' synergy over a mediterranean city. Environ. Res. 182, 109102.
Rui, L., Buccolieri, R., Gao, Z., Gatto, E., Ding, W., 2019. Study of the effect of green quantity and structure on thermal comfort and air quality in an urban-like residential district by ENVI-met modelling. In: Building Simulation, vol. 12, Springer, pp. 183–194.
Sailor, D., Anand, J., King, R., 2021. Photovoltaics in the built environment: A critical review. Energy Build. 253, 111479.
Salamanca, F., Georgescu, M., Mahalov, A., Moustaoui, M., Martilli, A., 2016. Citywide impacts of cool roof and rooftop solar photovoltaic deployment on near-surface air temperature and cooling energy demand. Bound.-Layer Meteorol. 161, 203–221.
Salamanca, F., Georgescu, M., Mahalov, A., Moustaoui, M., Wang, M., 2014. Anthropogenic heating of the urban environment due to air conditioning. J. Geophys. Res.: Atmospheres 119 (10), 5949–5965.
Salamanca, F., Krpo, A., Martilli, A., Clappier, A., 2010. A new building energy model coupled with an urban canopy parameterization for urban climate simulations—part I. formulation, verification, and sensitivity analysis of the model. Theor. Appl. Climatol. 99, 331–344.
Salamanca, F., Martilli, A., 2010. A new building energy model coupled with an urban canopy parameterization for urban climate simulations—Part II. Validation with one dimension off-line simulations. Theor. Appl. Climatol. 99 (3), 345–356.
Salmond, J.A., Tadaki, M., Vardoulakis, S., Arbuthnott, K., Coutts, A., Demuzere, M., Dirks, K.N., Heaviside, C., Lim, S., Macintyre, H., et al., 2016. Health and climate related ecosystem services provided by street trees in the urban environment. Environ. Heal. 15, 95–111.
Samaro, N., Hartmann, T., Baba, F., 2024. Overheating risks and mitigation strategies for an archetype residential building in hot climate zone under future conditions.
Santamouris, M., 2001. The role of green spaces. In: Energy and climate in the urban built environment. James & James Science London, pp. 145–159.
Santamouris, M., 2019. Mitigating the local climatic change and fighting urban vulnerability. In: Minimizing Energy Consumption, Energy Poverty and Global and Local Climate Change in the Built Environment: Innovating to Zero. Elsevier Amsterdam, The Netherlands, pp. 223–307.
Santamouris, M., 2023. Urban climate change: reasons, magnitude, impact, and mitigation. In: Urban Climate Change and Heat Islands. Elsevier, pp. 1–27.
Santamouris, M., Ding, L., Fiorito, F., Oldfield, P., Osmond, P., Paolini, R., Prasad, D., Synnefa, A., 2017. Passive and active cooling for the outdoor built environment–Analysis and assessment of the cooling potential of mitigation technologies using performance data from 220 large scale projects. Sol. Energy 154, 14–33.
Sharma, A., Conry, P., Fernando, H., Hamlet, A.F., Hellmann, J., Chen, F., 2016. Green and cool roofs to mitigate urban heat island effects in the Chicago metropolitan area: Evaluation with a regional climate model. Environ. Res. Lett. 11 (6), 064004.
Simpson, C.H., Brousse, O., Taylor, T., Grellier, J., Taylor, J., Fleming, L.E., Davies, M., Heaviside, C., 2024. Modeled temperature, mortality impact and external benefits of cool roofs and rooftop photovoltaics in London. Nat. Cities 1–9.
Skamarock, W.C., Klemp, J.B., Dudhia, J., Gill, D.O., Liu, Z., Berner, J., Wang, W., Powers, J.G., Duda, M.G., Barker, D.M., et al., 2019. A Description of the Advanced Research WRF Model Version 4, vol. 145, (no. 145), National Center for Atmospheric Research, Boulder, CO, USA, p. 550.
Skamarock, W., Klemp, J., Dudhia, J., Gill, D., Liu, Z., Berner, J., Wang, W., Powers, J., Duda, M., Barker, D., et al., 2021. A description of the advanced research WRF version 4.3,(No. NCAR/TN-556+ STR).
Statistical Service of Cyprus, 2023. Census of population. URL https://cystatdb.cystat.gov.cy/pxweb/en/8.CYSTAT-DB/8.CYSTAT-DB_Population_Census%20of%20Population%20and%20Housing%202021_Population_Population%20-%20Place%20of%20Residence/1891113E.px/table/tableViewLayout1/.(Accessed 10 October 2024).
Stone, Jr., B., Lanza, K., Mallen, E., Vargo, J., Russell, A., 2023. Urban heat management in Louisville, Kentucky: A framework for climate adaptation planning. J. Plan. Educ. Res. 43 (2), 346–358.
Stone, Jr., B., Mallen, E., Rajput, M., Broadbent, A., Krayenhoff, E.S., Augenbroe, G., Georgescu, M., 2021. Climate change and infrastructure risk: Indoor heat exposure during a concurrent heat wave and blackout event in Phoenix, Arizona. Urban Clim. 36, 100787.
Tewari, M., Yang, J., Kusaka, H., Salamanca, F., Watson, C., Treinish, L., 2019. Interaction of urban heat islands and heat waves under current and future climate conditions and their mitigation using green and cool roofs in New York City and Phoenix, Arizona. Environ. Res. Lett. 14 (3), 034002.
Tymvios, F., Charalambous, D., Michaelides, S., Lelieveld, J., 2018. Intercomparison of boundary layer parameterizations for summer conditions in the eastern Mediterranean island of Cyprus using the WRF-ARW model. Atmos. Res. 208, 45–59.
Tzyrkalli, A., Economou, T., Lazoglou, G., Constantinidou, K., Hadjinicolaou, P., Lelieveld, J., 2024. Urban heat island trends in the Middle East and North Africa: A statistical approach. Int. J. Climatol. 44 (11), 3998–4008. http://dx.doi.org/10.1002/joc.8563, arXiv:https://rmets.onlinelibrary.wiley.com/doi/pdf/10.1002/joc.8563, URL https://rmets.onlinelibrary.wiley.com/doi/abs/10.1002/joc.8563.
Viguié, V., Lemonsu, A., Hallegatte, S., Beaulant, A.L., Marchadier, C., Masson, V., Pigeon, G., Salagnac, J.L., 2020. Early adaptation to heat waves and future reduction of air-conditioning energy use in Paris. Environ. Res. Lett. 15 (7), 075006.
Vos, P.E., Maiheu, B., Vankerkom, J., Janssen, S., 2013. Improving local air quality in cities: to tree or not to tree? Environ. Pollut. 183, 113–122.
Wang, L., Huang, M., Li, D., 2020. Where are white roofs more effective in cooling the surface? Geophys. Res. Lett. 47 (15), e2020GL087853.
Watson, R.T., Core writing team, et al., 2001. Climate Change 2001: Synthesis Report, vol. 398, Cambridge University Press Cambridge.
Wong, N.H., Tan, C.L., Kolokotsa, D.D., Takebayashi, H., 2021. Greenery as a mitigation and adaptation strategy to urban heat. Nat. Rev. Earth & Environ. 2 (3), 166–181.
Zhao, Q., Sailor, D.J., Wentz, E.A., 2018. Impact of tree locations and arrangements on outdoor microclimates and human thermal comfort in an urban residential environment. Urban For. & Urban Green. 32, 81–91.
Zinzi, M., Agnoli, S., 2012. Cool and green roofs. An energy and comfort comparison between passive cooling and mitigation urban heat island techniques for residential buildings in the Mediterranean region. Energy Build. 55, 66–76.
Zittis, G., Almazroui, M., Alpert, P., Ciais, P., Cramer, W., Dahdal, Y., Fnais, M., Francis, D., Hadjinicolaou, P., Howari, F., et al., 2022. Climate change and weather extremes in the Eastern Mediterranean and Middle East. Rev. Geophys. 60 (3), e2021RG000762.
Zittis, G., Bruggeman, A., Camera, C., 2020. 21st century projections of extreme precipitation indicators for Cyprus. Atmosphere 11 (4), 343.
Zittis, G., Bruggeman, A., Camera, C., Hadjinicolaou, P., Lelieveld, J., 2017. The added value of convection permitting simulations of extreme precipitation events over the eastern Mediterranean. Atmos. Res. 191, 20–33.
Zittis, G., Hadjinicolaou, P., 2017. The effect of radiation parameterization schemes on surface temperature in regional climate simulations over the MENA-CORDEX domain. Int. J. Climatol. 37 (10), 3847–3862.
Zittis, G., Hadjinicolaou, P., Almazroui, M., Bucchignani, E., Driouech, F., El Rhaz, K., Kurnaz, L., Nikulin, G., Ntoumos, A., Ozturk, T., et al., 2021. Business-as-usual will lead to super and ultra-extreme heatwaves in the Middle East and North Africa. Npj Clim. Atmospheric Sci. 4 (1), 20.
Zölch, T., Maderspacher, J., Wamsler, C., Pauleit, S., 2016. Using green infrastructure for urban climate-proofing: An evaluation of heat mitigation measures at the micro-scale. Urban For. & Urban Green. 20, 305–316.
Zonato, A., Martilli, A., Gutierrez, E., Chen, F., He, C., Barlage, M., Zardi, D., Giovannini, L., 2022. Exploring the role of rooftop urban mitigation strategies in thermal comfort and energy consumption. Authorea Preprint.